# PERFORMANCE ANALYSIS AND MODELLING OF DIESEL ENGINE OPERATIONAL CHARACTERISTICS USING PYROLYTIC OIL FROM SCRAP TYRE

**By**

Maube Obadiah Mwanzi

(201324564)

**A thesis submitted in fulfilment of the requirements for the award of**

**Doctor of Technology in Mechanical Engineering**

**at Vaal University of Technology**

Promoter: Prof. A.A. Alugongo,

Co – Promoter: Prof L.M. Masu,

July 2017

.

# DECLARATION

I hereby, declare that this thesis is my original work and that it has not been submitted to any

other university or institution for a similar or any other degree award.

**Obadiah Maube**

## Dedication

I dedicate this work to my family and friends for their love and encouragement

## Acknowledgement

**Abstract**

In this work, an investigation on the fraction of tyre pyrolysis oil with a similar distillation range to that of automotive diesel (150 – 360 ºC) was carried out to determine its suitability as an alternative or additive to petro-diesel fuel. The quality of this oil was evaluated by comparing its key properties to the requirements of South African National Standards for Automotive diesel fuel (SANS-342) and to conventional automotive diesel fuel. The viscosity, density, copper strip corrosion of this fuel were found to be within the acceptable limits set by SANS while sulphur content and flash point were out of their respective set limits. In addition, mixing rule equations for predicting viscosity and density for both pure and blends of the oil as a function of temperature were developed and evaluated. The equations were found to be suitable due to their low Absolute Percentage Deviation. Engine performance tests were carried out with blends of Distilled Tyre Pyrolysis Oil (DTPO) and petro-diesel fuel in a single cylinder air cooled diesel engine. The performance, emission and combustion characteristics of the diesel engine while running on these blends were evaluated and subsequently, a comparative analysis was performed with conventional petro-diesel fuel as the reference fuel. It was found that, the engine could run with up to 60% (DTPO) without any problem. Beyond this level the engine became unstable. The power and torque were similar at low and medium speeds. However, at high speeds, the power dropped with increase in DTPO in the blend. Fuel consumption was very comparable for all the test fuels. Carbon monoxide and unburned hydrocarbons were higher for the blends compared to petro-diesel fuel but oxides of Nitrogen were lower. The peak pressure for petro-diesel fuel was marginally higher than that of the blends. Present results indicate that, petro-diesel fuel can be blended with up to 60% DTPO and produce acceptable performance. Testing the diesel engine under different operating conditions is a time consuming and expensive process that also requires the use of specialised equipment which may not be readily available. An Artificial Neural Network (ANN) model

based on a back-propagation learning algorithm was developed to predict engine performance and emissions separately, based on fuel blend and speed. The performance and accuracy of the model were evaluated by comparing experimental and ANN predicted results. The ANN was able to predict both engine performance and emissions with acceptable levels of accuracy. The values of correlation coefficient between experimental and predicted data being greater than 0.99. From this work, it can be implied that engine emission and performance can be predicted using neural network-based mode, consequently, it will be able to do further investigations without running laboratory experiments. Energy recovery from waste is an interesting field for engineers and scientists. It is hoped that this work will prompt new research ideals on how tyre pyrolysis oil can be improved for use as diesel engine fuel and building better models for diesel engine performance and emissions.

# Table of content

## List of tables

## List of figures

**List of acronyms**

| | |
|---|---|
| ANN | artificial neural network |
| APD | average percentage deviation |
| BDC | bottom dead centre |
| b | bias |
| BP | brake power |
| BSFC | brake specific fuel consumption |
| BSEC | brake specific energy consumption |
| BTE | brake thermal efficiency |
| CO | carbon monoxide |
| CNG | compressed natural gas |
| DEE | diethyl ether |
| DF | diesel fuel |
| DTPO | distilled tyre pyrolysis oil |
| FP | friction power |
| HC | hydro carbons |
| IP | indicated power |
| JME | jatropha methyl ester |
| $NO_X$ | Nitrogen oxides |
| MAPE | mean absolute percentage error |
| ME | mechanical efficiency |
| MSE | mean square error |
| MLP | multi-layer perceptron |
| PM | particulate matter |
| PPM | parts per million |
| R | correlation coefficient |
| $R^2$ | coefficient of determination |
| RMSE | root mean square error |
| RPM | revolutions per minute |
| REDISA | Recycling and Economic Development Initiative of South Africa |
| SA | South Africa |
| SANS | South Africa national standards |
| SSE | sum of squares error |
| TDC | top dead centre |
| TPO | tyre pyrolysis oil |
| W | weight |
| $W_{sr}$ | weight where $s$ indicates the destination and $r$ indicates the source |

# 1  INTRODUCTION

## 1.1  Background

Waste tyre disposal poses challenges especially with the tight regulations being put in place by environmental protection agencies. Tyres contain carbon black, steel cords, polyester and nylon fibre, steel bead wire, chemicals and fillers and up to 47% rubber/elastomers (Anne & Russ, 2006). Most of the tyre is composed of thermosetting polymers (Williams, 2013). Scrap tyres are difficult to recycle into other components because of their properties (Martínez *et al.*, 2013). In South Africa, it is approximated that 60 million tyres are scattered all over the country and 11 million add to this figure every year (Recycling and Economic Development Initiative of South Africa (REDISA), (2004)). The use of landfills in disposing of tyres is not ideal since they occupy a lot of space and tyres cannot be compacted unlike other land fill materials. Tyres take 80 to 100 years to biodegrade, since they are designed to endure severe operational environments (Martínez *et al.*, 2013).  Although landfills have been used in South Africa (SA) before, it is being discouraged due to environmental concerns associated with them and the space is also becoming scarce. This has led to illegal dumping or burning to recover the steel contained in tyres (Nkosi *et al.*, 2013). With South Africa importing most of its oil products, one way of dealing with the tyre disposal problem could be through pyrolysis of scrap tyres to produce oil that can be used as fuel. A study carried out in Gauteng province of South Africa revealed that the province alone has a potential of setting up a tyre pyrolysis industry that can produce up to 46.8 million litres of refined Tyre Pyrolysis Oil (TPO) per annum besides other valuable products derived from tyre pyrolysis (Pilusa *et al.*, 2014). The use of pyrolysis has increased since it provides a means of dealing with the waste tyre problem while recovering energy.

Internal combustion engines have been a popular source of power for various activities due to their portability, versatility and high power/volume ratio. Of the two types of internal combustion engines, the diesel engine is preferable because it has higher thermal efficiency compared to that of the petrol engine (Richard, 1992). With the rapid economic and population growth, there has been a huge demand for this engine as a source of power for automotive, agricultural machines, power generation, and home use equipment such as lawnmowers amongst other uses. This engine is powered by petro-diesel fuel derived from distillation of crude oil. This has in turn increased the demand for petro-diesel fuel whose sources are limited. In South Africa for example, the demand for petro-diesel fuel increased from 11,262 million litres in 2012 to 11,890 litres in 2013, which equates to an approximate 6% increase (http://www.sapia.co.za/publications/annual-reports.html). This demand can only increase further while the reserves remain finite. Throughout the world, the need to supplement conventional sources of fuel has led researchers to look for alternatives. Some of these alternatives include; biodiesel, alcohols such as ethanol, methanol, hydrogen, compressed natural gas and tyre pyrolysis oils.

The study of tyre pyrolysis oil (TPO) as fuel for the diesel engine has been on the rise since it provides a way of disposing of used tyres as well as energy recovery (Martínez *et al.*, 2013). Pyrolysis has been defined as "the thermal degradation of the organic components of tyres at typical pyrolysis temperatures to produce oil, gas and char products in addition to the recovery of steel" (Williams, 2013). During tyre pyrolysis, it is mainly the rubber that breaks down to low molecular weight products such oil and gas (Murugan *et al.*, 2009). Yields of up to 60% oil have been reported at optimum conditions of reactor time, temperature and particle size (Islam *et al.*, 2003). With a reported high energy content of up to 44 MJ/kg (Roy *et al.*, 1999), tyre pyrolysis oil presents a potentially good alternative as fuel for the diesel engine. Waste tyres can be an attractive source of feedstock for oil production since it is cheaply available,

given the vast quantities in dumpsites. Besides, the other products of pyrolysis such as char can have other economic values such as production of activated carbon, carbon black, solid fuel and pigment (de Marco Rodriguez *et al.*, 2001). The gas obtained during pyrolysis has a reported calorific value of 45 MJ/kg and could be used in gas motors for power production, or recycled back to the reactor for heating purposes (Frigo *et al.*, 2014).

Studies carried out using TPO in petro-diesel fuel have shown a significant difference in engine performance compared to petro-diesel fuel especially when blended with petro-diesel fuel in high concentration. These observations were attributed to the difference in properties of TPO compared to petro-diesel fuel (Aydın & İlkılıç, 2012, Martínez *et al.*, 2014, Sharma & Murugan, 2013, Frigo *et al.*, 2014, Doğan *et al.*, 2012, Hariharan *et al.*, 2013, Koc & Abdullah, 2014). These authors, cited above, used raw or distilled TPO without limiting it to a certain distillation range. In other words, the authors compared fuel with totally different boiling ranges, hence the difference in performance was expected. The observations included increased emissions, low thermal efficiency and power compared to petro-diesel fuel, in some cases the engines became unstable when the concentration of TPO in the TPO - petro-diesel fuel blend increased among others. Diesel engines were designed for petro-diesel fuel. Therefore, for a fuel to be compatible with the diesel engine the properties must be as close as possible to the petro-diesel fuel for optimum performance. Key properties of liquid fuels such as density, viscosity and Cetane number can be correlated to distillation characteristics of the fuel.

Crude oil, from which petro-diesel fuel is derived is a complex mixture of hydrocarbons which are separated into groups with similar boiling ranges by fractional distillation (Demirbas, 2008). Similarly, TPO is a mixture of unrefined hydrocarbons with a wide boiling range of between 70 and 400 ℃ (Martínez *et al.*, 2013). Therefore, the compounds in tyre pyrolysis oil should be separated according to boiling temperature range and refined in order for it to be

suitable for a particular application (Murillo *et al.*, 2006). There is evidence that separating the fuel into distinct fractions based on their boiling range can make TPO suitable for specific applications. Öztop *et al.*, (2014) investigated the use of light oil fractions of tyre pyrolysis oil with an initial boiling point of 65 ℃ and final boiling point of 303 ℃ as fuel for the spark ignition engine. The light oil fuel had an octane rating that was higher than that of petroleum and was found to be able to be blended with up to 60% gasoline fuel without any problem in engine operation. Chaala & Roy (1996) found that heavy residue fraction of TPO with boiling point of above 350°C meets the requirements for production of good quality speciality coke. Pilusa & Muzenda (2013) found that the TPO fraction distilled at 250 ℃ exhibited properties close to those of petro-diesel fuel. de Marco Rodriguez *et al.* (2001) compared the distillation characteristic of TPO distilled between 150 ℃ and 370 ℃ to that of commercial petro-diesel fuel. Though the two fuels did not exhibit a similar pattern throughout, the authors recommended further research on this fraction in order to establish its potential as fuel for the diesel engine. Laresgoiti *et al.* (2004) studied the distillation characteristics of different fractions of oil derived from TPO to their corresponding petroleum fractions and also compared them to their standard specifications and requirements. They found that the fraction with similar boiling range to automotive diesel fuel (150-350 ℃) and Heating petro-diesel fuel (150-390 ℃) met the standard specifications for the products based on distillation behaviour. The fraction that resembles petrol (70-150 ℃) did not meet the required specification. Distillation data alone may not be conclusive on whether this fraction is suitable as fuel for diesel engines. Therefore, there is need for further examination of the viability of this fraction of TPO that resembles petro-diesel fuel.

Studying the behaviour and characteristics of a process may require modelling. After experimental evaluation of engine performance on this fuel, it may be necessary to develop a predictive model for engine performance. Modelling provides a way of simulating and

understanding the engines response to different input parameters and conditions. The idea of modelling diesel engine operational parameters is not new. Analytical or mathematical methods have conventionally been used in modelling; however, they are time consuming due to the extensive computations involved (Ghobadian *et al.*, 2009). Numerous assumptions also have to be made in the course of modelling (Wong *et al.*, 2013, Richard, 1992, Ramos, 1989), thus they may not be realistic enough. This has led to the emergence of Artificial Intelligence Based Methods such as Artificial Neural Networks (ANN), which have been successfully used in various fields of engineering. The ANN is a mathematical model that was inspired by the biological neurons; it can receive inputs, perform operations and then predict final results or output, after training from experimental data (Yusaf *et al.*, 2011, Ghobadian *et al.*, 2009, Celik & Arcaklioğlu, 2005). The ANN can make predictions of numerous output variables based on several input parameters without prior knowledge of their relationship, through its ability to learn about the system that is being modelled (Ghobadian et al., 2009). This is done by training with experimental data and validation with independent data. ANN has been successfully used in modelling and simulation, performance prediction, fault diagnoses, performance monitoring and optimisation of diesel engine parameters with an acceptable degree of accuracy (Ghobadian *et al.*, 2009, Rawlins, 2005, Nikzadfar & Shamekhi, 2014, Taghavifar *et al.*, 2014, Jianmin *et al.*, 2011, Bietresato *et al.*, 2015, Roy *et al.*, 2014, Mohammadhassani *et al.*, 2015, Yusaf *et al.*, 2011).

## 1.2 Significance of the study

The variety of fuels being considered for use in the diesel engine is increasing due to the need of finding an appropriate substitute or supplement for the petro-diesel fuel. The properties of these fuels need to be examined and engine tests carried out to determine their suitability for use as alternative fuels for the diesel engine. It is well known that distillation range of a fuel

has effects on the fuel properties and in turn this may affect engine performance. Tyre pyrolysis oil has a wide distillation rage compared to diesel fuel. Therefore, it may be necessary to extract the fraction of TPO that resembles petro-diesel fuel based on distillation range (150 – 360 C) through fractional distillation and study of its technical feasibility as fuel for the diesel engine. After experimental evaluation, a model to relate engine input parameters to engine performance and emissions when the engine is running on TPO petro-diesel fuel blends, needs be developed based on Artificial Neural Network.

## 1.3    Statement of the problem

The typical distillation range of petro-diesel fuel is between 150 $^{\circ}$C and 360 $^{\circ}$C (de Marco Rodriguez *et al.*, 2001). 70% of TPO boils at less than 370 $^{\circ}$C which is similar to the upper limit set for petro-diesel fuel. However, the oil has a significant amount of low boiling point fractions (as low as 78 $^{\circ}$C) and hence, may not be suitable for use in the diesel engine in that state (de Marco Rodriguez *et al.*, 2001). The diesel engine was optimised for petro-diesel fuel fuel. There is therefore need to study the fraction of TPO that resembles petro-diesel fuel based on boiling range. No work could be found in literature regarding the study of Tyre Pyrolysis Oil which is similar to petro-diesel fuel based on distillation range (150 $^{\circ}$C and 360 $^{\circ}$C). In fact, de Marco Rodriguez *et al.* (2001) recommended research on this fraction in order to establish its real potential as fuel for the diesel engine.

With the increase of the use of internal combustion engines, along with the range of alternative fuels being used, scientists and engineers have paid a lot of attention to modelling engine characteristics (Nikzadfar & Shamekhi, 2014).  Testing the diesel engine under different operating conditions is a time consuming and an expensive process that also requires the use of specialised equipment which may not be easily available. This may not always be convenient. A technique that can make this prediction without running engine tests can be very

convenient. Thus, it is necessary to develop a model that can predict the engine performance using ANN.

## 1.4    Objectives

To analyse and model the performance and emission characteristic of a diesel engine operating on distilled tyre pyrolysis oil with a distillation range of between 150 ºC to 360 ºC.

### 1.4.1    Specific objectives

1. To extract the fraction of tyre pyrolysis oil that resemble petro-diesel fuel through fractional distillation.
2. To characterise the oil sample according to the relevant standards.
3. To perform engine tests with the oil and its blends with petro-diesel fuel.
4. To model the performance of an engine running on Distilled Tyre Pyrolysis Oil and its blends with petro-diesel fuel.

## 1.5    Scope of the study

This study focuses on the technical feasibility of using the fraction of TPO that resembles diesel fuel based on distillation range as diesel fuel, and to develop a model that predicts engine performance when running on this fuel using ANN.

## 2 LITERATURE REVIEW

### 2.1 The diesel engine

The diesel engine is a popular engine choice in economic activities compared to the petrol engine. Its preference is because it is more robust and has a high thermal efficiency compared to the Spark Ignition (SI) engine (Hansdah *et al.*, 2013, Celik & Arcaklioğlu, 2005). Richard (1992) gave three reasons for the higher thermal efficiency; it has a higher compression ratio than petrol engines, only air is present in the cylinder during initial compression and the air/fuel mixture is always lean. Besides that, Hydrocarbons (HC) and carbon monoxide (CO) emissions of the diesel engine are lower compared to SI engines, but its particulate matter (PM) and nitrogen oxides ($NO_x$) emissions are higher (Belagur & Wadawadagi, 2009).

### 2.2 Historical overview of the diesel engine

Rudolph Diesel developed the diesel engine with the aim of replacing steam engines. Initially it was to run on coal dust, but this ideal was later abandoned in favour of oil. In 1892 he filed a patent and ran the first model in 1893 with a remarkable efficiency of 26%. The first model suitable for practical use was demonstrated in 1897 and ran on peanut oil. Due to the size of the injector pump, the early engines were only suitable for large stationery and marine applications (Encyclopaedia Britannica, 1974). It was only during the 1920s that smaller high-speed diesel engines were developed for automotive use (Richard, 1992). With the development of drilling technologies there was cheap and abundant fossil fuel available. But after the 1973 fuel crisis, research intensified on the diesel engine, initially to design procedures and gadgets that could improve on efficiency such as vehicle aerodynamics, turbochargers, and intercoolers and consequently reduce fuel consumption. Recently, research has focused on identifying alternative fuels that could supplement petroleum sources while complying with the stringent environmental and legislative requirements.

### 2.2.1    Principle of operation of the diesel engine

The diesel engines can be classified as two stroke, where the engine requires two strokes of the piston to complete its cycle and the four stroke, where four strokes are required to complete a cycle. Diesel engines are commonly four stroke engines. The principle of operation of the diesel engine is described by Eastop & McConkey (1993) as follows: The four strokes consist of induction, compression, working and exhaust stroke. In the induction stroke, the valves open and air is induced into the cylinder as the piston moves from the Top Dead Center (TDC) to the Bottom Bead Dead Center (BDC). The second stroke is the compression stroke, here the valves close and the piston moves towards the TDC, thus compressing the air. Just before reaching the TDC fuel is injected into the chamber, mixes with the hot air and ignites. This combustion creates an expansion that pushes the piston down towards the BDC thus creating the working stroke. Finally, the valves open as the piston moves upwards, discharging the products of combustion. This is the final stage also known as exhaust stroke.

### 2.2.2    Performance parameters of an internal combustion engine

To evaluate engine performance, certain quantities are measured through bench tests at different speeds and loads. Then calculations are performed using standard procedures. The results are presented graphically in form of performance maps. The following is an overview of the key parameters as described by Eastop & McConkey, (1993) and Richard (1992).

1. Indicated power (IP) – is the rate at which work is done on the piston in the cylinder. It is given by 2.1

$$IP = \frac{p_i ALNn}{2} \qquad \qquad 2\text{-}1$$

Where $p_i$ is the indicated mean effective pressure, and is determined from the engines indicator diagram. A and L are area and length of the cylinder respectively. N is the number of cycles per unit time while n is the number of cylinders.

2. Brake Power (BP) – this is the useful power as measured from the output shaft by a dynamometer. Brake power is calculated by 2.2.

$$BP = 2\pi NT \qquad\qquad 2\text{-}2$$

Where T is torque developed by the engine

3. Friction Power (FP) and Mechanical efficiency (ME) - the difference between the IP and BP is accounted for as power to overcome friction. Hence friction power (FP). ME is the ratio of BP to IP, usually expressed as a percentage and it normally lies between 80 and 90%.

$$FP = IP - BP \qquad\qquad 2\text{-}3$$
$$ME = \frac{BP}{IP} \, x \, 100 \qquad\qquad 2\text{-}4$$

4. Brake Thermal Efficiency (BTE) – this is the overall efficiency of the engine. It's a criterion that evaluates how efficiently the chemical energy of the fuel is converted to mechanical energy.

$$BTE = \frac{BP}{mass\ flow\ rate\ of\ fuel \times calorific\ value} \quad 2\text{-}5$$

5. Brake Specific Fuel Consumption (BSFC) – this is Measure of the mass of fuel consumed per unit BP produced by the engine; it is a criteria used to evaluate the engines fuel economy. Its units are kg/kWh. A lower BSFC of the engine is desired since it shows the better fuel economy.

$$BSFC = \frac{mass\ flow\ rate}{BP} \qquad 2\text{-}6$$

6. Engine Emissions – these are pollutants available in the exhaust fumes. These emissions include carbon monoxide (CO), oxides of nitrogen ($NO_x$), unburned hydrocarbons (HC) Sulphur dioxide ($SO_2$) and soot.

### 2.2.3   Combustion process in the diesel engine

The combustion process in a compression ignition can be divided into four stages as follows (Benson & Whitehouse, 1983, Richard, 1992): The first stage is the Ignition Delay, this is the period between the start of fuel injection and when the first fuel droplets start to ignite. It is during this period that the fuel will atomise, vaporise and mix with air. This is followed by the next stage of rapid and uncontrolled combustion. The pressure rises rapidly to a maximum point due to combustion caused by the ignition of the prepared air/fuel mixture during the ignition delay stage. The third stage starts after the air/fuel mixture that was prepared during the ignition delay is exhausted.  The rate of combustion at this stage is now determined by the fresh air/fuel mixture induced into the cylinder. In the final stage, the rate of combustion is low until all the air or fuel is exhausted. Ignition delay hugely determine the smoothness of engine operation and emissions. Figure 2-1 shows the pressure vs crank angle diagram for a compression ignition engine.
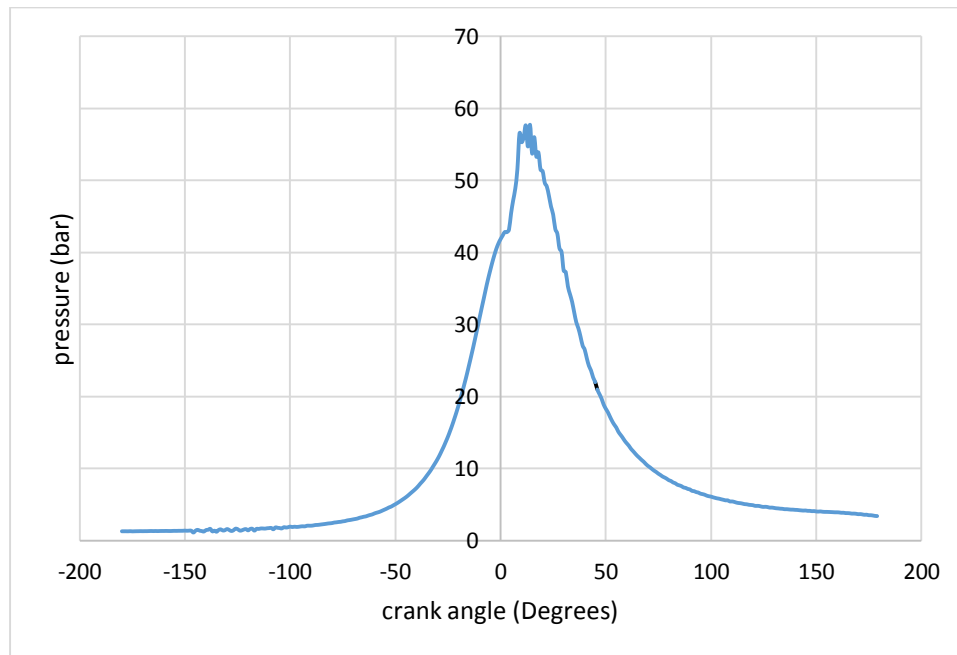
Figure 2-1 Pressure diagram of a compression ignition engine

### 2.2.4 Fuels and compression ignition engines

Liquid fuels hold huge quantities of energy per unit volume compared to solid and gaseous fuels. Together with the ease of handling and combustion characteristics, they have become an appealing source of energy. A variety of fuels have been investigated as for their suitability as fuel for the internal combustion engine.

Alcohols such as bioethanol (Hansdah *et al.*, 2013) n-butanol (Siwale *et al.*, 2013) and methanol (Yasin *et al.*, 2014) have also been extensively studied. Their limitation is their low Cetane number and viscosity, therefore, they have to be blended with petro-diesel fuel before they can be used in the internal combustion engine. Another challenge is that they do not remain in one phase after blending, especially over a wide range of temperatures. They can only be used in small quantities in blends with petro-diesel fuel or biodiesel and produce acceptable performance. The effects of introducing hydrogen as a secondary fuel through the air inlet manifold on an engine running on petro-diesel fuel was investigated by Dhole *et al.* (2014). Compared to pure petro-diesel fuel, there was an increase in brake thermal efficiency,

Unburned Hydrocarbon (HC) and carbon monoxide (CO). $NO_x$ was found to be lower. The authors observed that 20% substitution of hydrogen in petro-diesel fuel offered the best performance. Yusaf *et al.* (2010) found that an engine running on Compressed Natural Gas CNG-diesel offers better brake thermal efficiency and lower emissions. The problem with the use of hydrogen is that extensive modification had to be made on the engine to make it suitable for this fuel. The modifications included; changing compression ratio, modifying the diesel injection system, installing CNG injection system and modifications on the air manifold and inlet valve. Biodiesel has proved to be an attractive fuel mainly because of the following reasons; it can be domestically produced, inherent lubricity, it is biodegradable; low particulate, CO, HC, soot and in some conditions $NO_x$ compared to petro-diesel fuel, contains no Sulphur; compatible with diesel engine amongst others (Ghobadian *et al.*, 2009, Canakci *et al.*, 2009, Demirbaş, 2008). Of the possible alternatives so far, biodiesel is the most attractive since it can run in the diesel engine without any modification. Tyre pyrolysis has also been investigated and will be discussed in detail in the later sections.

### 2.2.5   Petro-diesel fuel

Crude petroleum is an unrefined mixture of hydrocarbons and a small proportion of non-hydrocarbons. The hydrocarbons include alkanes (paraffins), cycloalkanes (naphthenes), aromatics and Naphtheoaromatics (complex hydrocarbons) while the non-hydrocarbons include sulphur, oxygen, nitrogen and metallic compounds (Neumann et al., 1981). Crude oil consists of components with wide boiling range. So during petroleum refining, the crude oil is separated into components within a desired boiling range before undergoing further treatment to make it suitable for specific applications. As shown in Table 2-1 and described by Neumann et al. (1981), the first three fractions of crude oil are distilled under atmospheric conditions. The light fuel oil consists of fractions with boiling range of between 30 ºC to 100 ºC and 100 ºC to 200 ºC. The residue with boiling range above 350 ºC is normally distilled under vacuum

conditions, then the distillation value is converted to standard pressure. The oil produced in this distillation range is suitable for use as lubrication oil and asphalt.

Table 2-1 Distillative separation of crude oil (Source: Richard 1992)

| | Crude oil | | | | | | |
|---|---|---|---|---|---|---|---|
| | Distillation under atmospheric pressure | | | | Atmospheric residue | | Vacuum residue |
| Fraction | gas | Gasoline light | Gasoline heavy | Gas oil | Vacuum distillate | | |
| Boiling range ºC | -162 to 30 | 30 to 100 | 100 to 200 | 200 to 350 | 350 to 450 | 450 to 550 | |
| Technical products | Liquefied petroleum gas | | Feed for petro-chemistry | Petro-diesel fuel | Feed for catalytic cracker | Lubrication oil | asphalt |
| | | Gasoline | | Fuel oil light | Fuel oil heavy | | |

## 2.3 Tyre pyrolysis

### 2.3.1 Tyre composition

Anne & Russ (2006) reported that a new tyre weighing approximately 10 kg manufactured by Goodyear contains up to 30 types of synthetic rubber, 8 types of natural rubber and carbon black, cords, wires, fibres and other additives and ingredients. The composition of passenger, lorry and off -road (ORT) tyre as reported by the authors is summarised in Table 2-2.

Table 2-2 Composition of Passenger, lorry and off road tyre. (Source: Anne & Russ, 2006)

| Constituent | Passenger car tyre (% weight) | Lorry tyre (% weight) | Off read tyre (% weight) |
|---|---|---|---|
| Rubber/elastomers | 47 | 45 | 47 |
| Carbon black | 21.5 | 22 | 22 |
| Metal | 16.5 | 25 | 12 |
| Textile | 5.5 | - | 10 |
| Zinc oxide | 1 | 2 | 1 |
| Sulphur | 1 | 1 | 1 |
| Additives | 7.5 | 5 | 6 |

## 2.3.2 Tyre pyrolysis oil production and yield

Pyrolysis is defined as the thermal degradation of organic components in the absence of air, yielding liquid (oil), gas and solid (char) fractions (Williams, 2013, Alcala & Bridgwater, 2013, Edwin Raj *et al.*, 2013). Pyrolysis has been studied with conditions being varied with the aim of maximising on the oil yield. These conditions are discussed in this section and summarised in Table 2-3.

Table 2-3 Reported yield at various operation conditions

| Reference | Feed stock, reactor type and operating conditions | Optimum oil Yield % | | |
|---|---|---|---|---|
| | | Oil | char | gas |
| (Islam *et al.*, 2003) | 5-7 cm tire particles externally heated in a fixed bed reactor. Temperature of $450°C$ . N$_2$ was used as a carrier gas. | 61 | 30 | 9 |
| (Murugan *et al.*, 2008a) | Tyre chips from the periphery of the tyre were fed into fixed bed reactor, heated externally in the absence of oxygen. Process carried out between temperature range of 450 and $650°C$ at constant heating rate of $5 °C /min$ and 120 min residence time. | 55 | 34 | 10 |
| (Murugan *et al.*, 2008b) | Tyre chips with bead, steel and fabric removed. Pyrolysis carried out in a vacuum and reactor was externally heated. Temperature between $450 – 650°C$. and residence time of 90 minutes | 50 | 40 | 10 |
| (Aydın & İlkılıç, 2012) | Reaction performed at temperature range of $400 – 700 °C$ in increments of $100°C$ and at various N$_2$ flow rates. Highest liquid yield observed at $500°C$ . the effect of N$_2$ flow rate was negligible | 40.26 | 47.88 | 11.86 |

| (Banar *et al.*, 2012) | Carried out at atmospheric pressure and temperature of between 350ºC and 600ºC in 50ºC increments in a fixed bed reactor. Heating rate was 5 and 35ºC/min. The highest yield was obtained at 400ºC and 5ºC/min. | 38.8 | 27.2 | 34 |
|---|---|---|---|---|
| (Frigo *et al.*, 2014) | Carried out in an externally heated pilot scale reactor at Temperature range of between $300 - 500°C$ at various crushed tyre flow rate. | 45 | 50 | 5 |
| (Martínez *et al.*, 2014) | Granulated tyres fed in a continuous auger reactor at feed rate of about 6.7 kg/h. reaction temp of 550ºC, $N_2$ used as carrier gas at 5 L/min. Residence time 3 min. | 42.6 | 40.5 | 16.9 |

Younus *et al.* (2013) carried out pyrolysis on automobile tyres between temperatures of 450 ℃ and 650 ℃ for a duration of 2 hours and 30 minutes. The yield from the process was 50% TPO, 40% pyro gas and 10% char by weight. The authors found that around 7.8 MJ/kg of energy was required for the process. Martínez *et al.* (2014) produced tyre pyrolysis oil from truck, tractor and car tyres in a continuous auger reactor. The reaction was done at optimum reactor conditions of 550 ℃ and 1 bar. The feedstock residence time was 3 minutes and flow rate was 6.7 kg/h. The liquid, solid and gas yields were found to be about 42.6 %, 40.5 % and 16.9 % by weight respectively. Effects of tyre particle size, running time and reactor temperature on yield was investigated by Islam *et al.* (2003) in a fixed bed reactor with nitrogen gas as a carrier gas. Tyre particle size of $5 - 7$ cm was found to have a higher oil yield compared to that with particle size of $1 - 4$ cm. The authors suggested that this could be because the smaller particles of tyre were blown out of the reactor before complete devitalisation. The authors also noted that the oil yield kept increasing with time. However, after 90 minutes' reaction time, the oil yield remained constant. This was because all the volatile fractions had

been exhausted. The reactor temperature was varied between 400 ℃ and 500 ℃. The optimum oil yield of 62% was obtained at a temperature of 450 ℃. At low temperatures, char content was higher but reduced with increase in temperature while the gas yield was low and increased with increase in temperature. This is because the low temperature was not sufficient for complete devitalisation resulting in high char and low oil and gas fractions. Banar *et al.* (2012) noted a 29.5% reduction in liquid yield when the temperature was increased from the optimum temperature of 400 $^{o}$C in that work to 600 $^{o}$C, while there was an increase in gas yield with increase in temperature beyond the optimum point. This is probably due to further cracking of the liquid to gas (Murugan *et al.*, 2008b, Williams, 2013, Banar *et al.*, 2012). In a similar work by Banar *et al.* (2012), the effects of increasing heating rate on yield was studied. It was found that a lower heating rate of 5 $^{o}$C/min had a higher oil yield of 38.8% compared to a heating rate of 35 $^{o}$C/min that yielded 31.1% oil. The influence of tyre brand on yield and composition of pyrolysis products was investigated by Younus *et al.* (2013). Seven brands of tyres from different manufacturers were used in this work using a fixed bed reactor under similar conditions. The yields of char (37.7 – 38.7% weight), oil (55.4 – 57.4 % weight) and gas (2.7 – 5 % weight) for the different brands were found to be very similar. However, there were differences in the composition of the products. The composition of gasses was found to vary with brand. There was similarity in their chemical composition, but the concentration of the compounds varied. There was also a variation of elemental composition of the oils with brand. Pyrolysis has to be carried out in an oxygen free environment. Therefore, a vacuum can be created or an inert gas such as $N_2$ may be used to prevent the tyre particles from burning due to the high temperatures in the reactor (Aydın & İlkılıç, 2012) and to carry away vapour from the reactor during the process (Islam *et al.*, 2003). Aydın & İlkılıç (2012) investigated the effects of $N_2$ flow rate on yield of pyrolysis products. The $N_2$ flow rate was adjusted from 150 cm$^3$/min to 350 cm$^3$/min in increments of 50 cm$^3$/min. The authors did not find any significant

differences in the yields of the products with change in flow rate. Catalytic pyrolysis was studied as a means of enhancing oil yield by Kar (2011). The author compared yield of catalytic and non-catalytic pyrolysis using expanded perlite as catalyst. The highest oil yield of non-catalytic pyrolysis was 60.02% by weight while that of catalytic pyrolysis was 65.11% by weight. This was a remarkable increment of 8.48% weight oil yield. Frigo *et al.* (2014) investigated the effect of varying crushed tyre flow rate in a continuous pilot scale reactor. The flow rates were varied between 5.5 kg/h and 14.5 kg/h. As flow rate increased, the solid yield was found to increase while the gas yield reduced. The oil yield kept increasing with increase in flow rate up to a maximum of 45% at 10 kg/h flow rate then started to drop. This reactor had different sections where the temperatures were varied between 300 $^{\circ}$C – 500 $^{\circ}$C. Edwin Raj *et al.* (2013) studied the effect of temperature, particle size and feed rate on yield in a fluidised bed reactor. They found that temperature was the most significant factor affecting oil yield. The highest oil yield in this study was obtained at 440 $^{\circ}$C.

### 2.3.3 Properties of tyre pyrolysis oil

There are several fuel properties that are critical for sound operation of the diesel engine. Some of these properties for TPO are shown in Table 2.4 and are discussed in the following section. Some authors have gone further to modify TPO by distillation. Distilled Tyre Pyrolysis oil (DTPO) has been found to have properties closer to petro-diesel fuel than raw TPO.

Table 2-4 Properties of TPO reported in literature

| Author | Density @ kg/m$^3$ | Heating Value | viscosity@40 $C°$ | Cetane number | Elemental analysis % | | | | |
|---|---|---|---|---|---|---|---|---|---|
| | | | | | C | H | O | N | S |
| (Islam *et al.*, 2003) | 971 @ 15 $C°$ | 41.7 | 4.8 | - | 80.30 | 5.18 | 10.13 | - | - |
| (Murugan *et al.*, 2008a) | 935@ 15 $C°$ | 42.8 (gross) | 3.2 | | - | - | - | - | 0.95 |
| (Murugan *et al.*, 2008a)[*] | 871 15 $C°$ | 45.6 (gross) | 1.7 | - | - | - | - | - | 0.03 |
| (Murugan *et al.*, 2008b) | .9239 15 $C°$ | 38 | 3.77 | - | 83.48 | 13.12 | 2.46 | 0.22 | 0.72 |
| (İlkılıç & Aydın, 2011) | 945 @ 20$C°$ | 43.34 | 3.8 | - | - | - | - | - | 0.9 |
| (Aydın & İlkılıç, 2012) | 0.945 @ 20$C°$ | 43.34 | 3.8 | 44 | 86.87 | 10.07 | 1.67 | 1.184 | 0.906 |
| (Bhatt & Patel, 2012) | 880 @ 15 $C°$ | 42.7 | 6.3 | 42 | - | - | - | - | - |
| (Banar *et al.*, 2012) | 820@ 15 $C°$ | 42.61 | 0.95 @50 $C°$ | | 68.91 | 9.6 | 18.37 | 2.05 | 1.07 |
| (Doğan *et al.*, 2012)* | 944.4 @ 15 $C°$ | 39.9 | 5.06 | - | - | - | - | - | - |

| (Doğan *et al.*, 2012) | 904 @ 15 $C°$ | 40.9 | 2.16 | - | - | - | - | - | - |
|---|---|---|---|---|---|---|---|---|---|
| (Hariharan *et al.*, 2013) | 935 15 $C°$ | 43.8 | 3.2 | - | 81.18 | 10.92 | 4.62 | 1.85 | 0.72 |
| (Sharma & Murugan, 2013) | 920 @ 20$C°$ | 39.2 | 5.4 | - | -- | - | - | - | - |
| (Frigo *et al.*, 2014) | 903 | 41.96 | 2.90 | - | - | - | - | - | 0.97 |
| (Martínez *et al.*, 2014) | 917 @ 15 $C°$ | 42.7 | 2.39 | | 86.19 | 10.33 | 0 | 0.79 | 0.83 |

*Distilled Tyre Pyrolysis Oil (DTPO)

### 2.3.3.1 Sulphur content

Literature reviewed has reported a significantly high Sulphur content in TPO compared to that of petro-diesel fuel and biodiesel. From Table 2-4, the sulphur content of TPO was from 0.72 to 1.07 ppm. Sulphur in TPO comes from the original feedstock. It is normally used to strengthen rubber in a process known as vulcanisation. Frigo *et al.* (2014) estimated that after pyrolysis, about 77% mass of the Sulphur in the tyre remains in the solid fraction while the remainder remains in the liquid fraction. The sulphur content of a fuel has significant effect on fuel emissions. It has been reported that (Tan *et al.*, 2013) exhaust smoke, HC, CO and $SO_2$ emissions reduced with reduction in sulphur content in the fuel whereas there was a remarkable decrease in particulate matter (PM) in the emissions. The authors explained that during combustion, sulphur is converted to $SO_2$, thus consuming part of the oxygen that could have otherwise oxidised CO and HC to $CO_2$ and $H_2O$. Sulphur reaction also leads to the formation of sulphates causing accumulation of carbon hence, soot formation. Apart from emission

concerns, sulphur can cause engine corrosion when exposed to high temperatures (Khan & Ali, 2013). For these reasons, Sulphur levels should be kept as low as possible. SANS 342:2006 recommends a maximum value of 500 ppm. Studies have been carried out in an attempt to reduce sulphur content of TPO. İlkılıç & Aydın (2011) investigated the effects of various rations of $Ca(OH)_2$ as a catalyst during pyrolysis on sulphur content of TPO. The optimum amount of catalyst was found to be 5% $Ca(OH)_2$. This reduced the sulphur content of raw oil by 34%. In a similar study (Aydın & İlkılıç, 2012), effects of using different catalysts such as $Ca(OH)_2$, $CaO$ and $NaOH$ were studied. It was reported that using 5% mass $Ca(OH)_2$ catalyst during pyrolysis then followed by acid desulphurisation using 10% $H_2SO_4$ with a degree of purity of 98% reduced sulfur content by a remarkable 83.75%. Koc & Abdullah (2014) reported a reduction of sulphur content of TPO from 0.768% to 0.321% in their study. The method used by the authors involved mixing TPO with a binary solution containing tetraoctylammonium bromide and HO, then exposing the solution to high intensity ultrasound for 5 minutes. Sulphur content has also been found to increase with pyrolysis reaction temperature. Aydın & İlkılıç (2012) found that oil obtained at 500 ℃ had 3% higher sulphur content compared to that obtained at 400 ℃.

### 2.3.3.2 Cetane number and Cetane index

This is a measure of the fuel's ability to auto ignite on compression and it has direct influence on the ignition delay. Therefore, it determines the ignition quality of a fuel. SANS 342:2006 recommend a minimum Cetane number of 45 while ASTM Standard D 975-02 recommends a minimum of 40. Typical petro-diesel fuels have Cetane numbers in the range of 45–50 (Hansen *et al.*, 2005). The diesel engines operate well with fuels that have a Cetane number in the range of 40 – 55 (Bhatt & Patel, 2012). Very little literature has reported on the Cetane number of TPO. However, from Table 2-4 the reported values of 42 and 44 are well within the above

reported range and ASTM D 975-02 specification, but lower than SANS 342:2006 recommended value. Higher Cetane number fuels have shorter ignition delay periods while low Cetane number fuels have longer ignition delay periods, thus delaying start of combustion (Hariharan *et al.*, 2013). Increase in Cetane number leads to a decline in PM and HC emissions (Tan *et al.*, 2013). Experimental determination of Cetane number is an expensive process, so sometimes a calculated value known as Cetane index (CI) is normally used to give an estimation of the Cetane number. However, this CI is only accurate when dealing with petroleum products rather than alternative fuels.

### 2.3.3.3 Density

The density of TPO is generally higher than that of petro-diesel fuel, though after distillation the density of DTPO approaches that of petro-diesel fuel (Tan *et al.*, 2013, Murugan *et al.*, 2008a). Density of the fuel is also another important parameter. Since fuel is metered to the diesel engine on volume basis, a fuel of high density has more mass per unit volume than a fuel of low density. Therefore, a fuel with high density is likely to produce more engine power than a fuel with low density. At high speeds and loads, this could be a problem. The petro-diesel fuel system is meant to inject the fuel on volume basis. Therefore, for the same volume a fuel with a larger density will have more fuel being injected into the combustion chamber. This will lead to a rich mixture, thus leading to smoke emission. SANS 342:2006 only sets a minimum limit of density at 800 kg/m$^3$. The upper limit is not set. The density of TPO is well above this value and higher than that of petro-diesel fuel. Another observation is that $NO_x$ emission increases with an increase in density (Hossain & Davies, 2013, Doğan *et al.*, 2012).

### 2.3.3.4 Viscosity

When a fuel is injected into the cylinder, it will break into droplets, mix with air and vaporise before combustion takes place. For proper combustion, the air-fuel mixture must be uniform.

The quality of spray, air -fuel mixing and distribution of fuel droplets in the cylinder determines the quality of combustion in the cylinder. This property is normally attributed to viscosity. From Table 2-4, the lowest reported viscosity of TPO is 2.39 cST, while most of the other reported values are higher than that of petro-diesel fuel. The highest reported value being 6.3 cST. This value is more than twice that of petro-diesel fuel at 2.79 cST (Martínez *et al.*, 2014). SANS 342:2006 limits the viscosity range of petro-diesel fuel to between 2.2 - 5.3 cST. High viscosity fuels also lead to longer ignition delay since it will result in poor atomisation, thus, more fuel-air mixture will be prepared during the premixed combustion phase (Murugan *et al.*, 2008b). Low viscosity leads to better fuel preparation during ignition delay leading to better combustion.

### 2.3.3.5   Heating value

The most important property of a fuel is the amount of energy produced during combustion. This is measured using the Heating Value or Calorific Value. It shows the amount of heat released per unit mass of fuel burned and it influences power and fuel consumption of the engine. From reported values in Table 2-4, TPO has a remarkable heating value of 38 – 44 MJ/kg. Though this is slightly lower than the reported value of petro-diesel fuel of 45.13MJ/kg (Martínez *et al.*, 2014). Carbon content in hydrocarbon fuel is an indicator of energy content of a fuel (Hariharan *et al.*, 2013). As seen in Table 2-4, TPO has lower carbon content compared to petro-diesel fuel and this explains the low energy content of TPO compared to that of petro-diesel fuel.

### 2.3.4   Engine performance

Research has been carried out to investigate the effects of using TPO on engine performance and emissions (Murugan *et al.*, 2008b, Frigo *et al.*, 2014, Hariharan *et al.*, 2013, Sharma & Murugan, 2013, Younus *et al.*, 2013). Petro-diesel fuel was used as the reference fuel so this

performance was being compared to that of TPO. Effects of blends of TPO with petro-diesel fuel, biodiesel and additives such as ignition improvers have been reviewed in this section.

Murugan *et al.* (2008b) prepared three blends of 10%, 30% and 50% TPO with petro-diesel fuel by volume and tested in a single cylinder stationary air cooled direct injection diesel engine. The results were reported at full load. The Brake Thermal efficiency was found to be 29.5, 27.2, 28.5 and 28.9% for petro-diesel fuel, TPO 10, TPO 30 and TPO 50 respectively. Among the blends, TPO 30 showed better performance at all loads. The CO, $NO_x$ and HC emissions for the blends were higher when the engine was running on the blends than when running on petro-diesel fuel. The CO concentration increased by an average of 12% compared to that of petro-diesel fuel. Apart from TPO 30, the rest of the blends exhibited high smoke emissions.

Frigo *et al.* (2014) compared blends of 5 - 45% TPO with petro-diesel fuel. There was no significant change in engine performance with blends containing up to 20% TPO compared to that of petro-diesel fuel. However, the engine became unstable when running on fuel with above 40% TPO concentration. Brake Specific Fuel Consumption (BSFC), Torque, Power output and emissions of an engine fuelled with blends of TPO and petro-diesel fuel were investigated by İlkılıç & Aydın (2011). In that study TPO was blended to 5 (TPO5), 10(TPO10), 15(TPO15), 25(TPO25), 35(TPO35) and 75% (TPO75) by weight with petro-diesel fuel. Engine power was found to reduce with increase in TPO concentration in the blend while the BSFC increased with increase in TPO concentration. The torque and engine power of TPO 100 was 11.86% and 16.6% lower than that of petro-diesel fuel while the BSFC of TPO was found to be 12% higher. HC and CO for TPO 100, 75 and 50 were much higher than those of lower blends (TPO 15, 25 and 35). $SO_2$ increased with increase in TPO concentration in the blend. This study concluded that blends of up to TPO 35 could be used in diesel engines

without engine modifications. TPO 50 -100 was found to be unsuitable due to the high CO, HC, $SO_2$ and smoke emissions. (Kumar *et al.*, 2012) also noted that a blend containing 20% TPO with diesel engine produced optimum performance in terms of thermal efficiency and BSFC while keeping emissions low.

The effects of TPO that has been improved by distillation on engine performance and emissions was studied by Doğan *et al.* (2012). The experiments were performed at full load and varying speed. Blends containing DTPO 10, 30, 50, 70 and 90% with petro-diesel fuel were prepared for this work. There was no significant difference in the torque and power output for up to 70% DTPO. There was no significant difference in Brake Specific Energy Consumption (BSEC) with blends of up to 50% DTPO. Beyond 50%, there was an increase in BSEC at medium loads. At low and high engine speeds, the thermal efficiency of the blends was higher than that of petro-diesel fuel. There was a tendency of $NO_x$, CO increasing with increase in DTPO concentration while the opposite trend was noted for HC, smoke opacity.

Effects of ignition improver, Diethyl Ether (DEE) as an additive to TPO on diesel engine performance was investigated by Hariharan *et al.* (2013). DEE was inducted into the engine through intake air at flow rates of 65g/h, 130g/h and 170g/h. HC, CO and smoke emissions were higher than that of petro-diesel fuel, but there was an improvement with increase in DEE flow rate. NOx was found to be lower than that of petro-diesel fuel. Due to the low Calorific Value of DEE, the thermal efficiency reduced while the BSFC increased with increase in DEE flow rate.

The use of TPO and Jatropha Methyl Ester (JME) blends on performance of the diesel engine has been investigated by Sharma & Murugan (2013). TPO from10% to 50% in increments of 10% by volume was blended with Jatropha Methyl Ester. JMETPO 20 exhibited the best performance. The thermal efficiency of this blend at high load was found to be close to that of

petro-diesel fuel while the BSEC was 7.8% higher than that of petro-diesel fuel at high loads. CO, HC and smoke emissions at full load were lower than those of petro-diesel fuel by 9.09, 8.6 and 26% respectively while $NO_2$ was 24% higher.

The use of ternary blends containing biodiesel, petro-diesel fuel and TPO in engine performance was investigated by Koc & Abdullah (2014). Five fuel samples were used in this study. B5D95, B10D90, B5T5D90, B10T10D80 and D100. B, T and D represent biodiesel, TPO and petro-diesel fuel respectively while the numeric value represent the percentage concentration. In terms of power, torque, fuel consumption and CO emissions, B10T10D80 exhibited better overall performance. B10T10D80 produced the highest power, torque and lowest fuel consumption compared to other blends. The authors suggested that future research need to focus on improving fuel properties with pre-treatment and identifying the ideal biodiesel, TPO and petro-diesel fuel blends that will produce optimum engine performance with reduced emissions.

The general observation was that tyre pyrolysis oil is not suitable for diesel engines without blends and additives. The higher the blend concentration the higher the emissions. The fuels with high TPO concentrations tended to produce lower torque and power. This could be due to the lower heating energy than that of petro-diesel fuel. Brake Specific Fuel Consumption (BSFC) is an indication of the mass required to produce a unit output of Brake Power. Using TPO, the same amount of power as the one produced by petro-diesel fuel was able to be achieved. However, due to the low energy content of TPO, more fuel will be required. This will lead to the reported high fuel consumption and low Brake thermal efficiency (BTE).

### 2.3.5 Combustion analysis of tyre pyrolysis oil

### 2.3.6 Ignition delay

TPO has a lower Cetane number and higher viscosity compared to that of petro-diesel fuel, thus the engine is expected to exhibit a longer ignition delay. Murugan *et al.* (2008b) reported an increased ignition delay with increase in TPO Petro-diesel fuel blends. This was attributed to the high viscosity of TPO and its blends compared to petro-diesel fuel. Hariharan *et al.* (2013) investigated the effect of DEE in ignition delay of an engine running on TPO. It was found that the ignition delay reduced with increase in quantity of DEE. The Cetane number of DEE (125) is much higher than that of petro-diesel fuel, therefore, it reduced the ignition delay period compared to that of petro-diesel fuel. Martínez *et al.* (2014) found that there was little difference between the ignition delay of TPO5 and that of petro-diesel fuel. This was attributed to the small difference in Cetane number and the lower viscosity of the fuel in this blend partly compensated with improved combustion. In another study (Sharma & Murugan, 2013) it was reported that an engine running on JME, JMETPO10 and JMETPO20 had a shorter ignition delay compared to that of petro-diesel fuel. This was attributed to the higher Cetane number of JME and the presence of oxygen in JME that resulted in improved reaction and combustion.

### 2.3.7 Cylinder peak pressure and rate of pressure rise

The peak pressure and the rate of pressure rise is linked to the ignition delay. The rate of pressure rise determines the smoothness of engine operation. A rapid rise will lead to vibrations while a slower pressure rise will lead to a smoother operation. When the ignition delay is long, a large amount of charge will accumulate in the cylinder during the ignition delay period. This will rapidly burn during the uncontrolled ignition leading to high peak pressure and rate of pressure rise. Blends of TPO and petro-diesel fuel have been found to have high peak pressure and higher rate of pressure rise compared to petro-diesel fuel. Blends of JMETPO have been

found to have a lower rate of pressure rise compared to petro-diesel fuel, apart from JMETPO 10 and 20, while the peak pressure increased with the quantity of TPO in the blend (Sharma & Murugan, 2013). JMETPO30 and JMETPO 50 had longer ignition delays due to reduction of CN with increase in TPO in the blend.

### 2.3.8   Analysis of Engine emissions

During combustion, exhaust emissions such as CO, $NO_x$, HC, $SO_2$, and particulates are formed as a result of incomplete combustion.

Unburned hydrocarbon (UBH) is an important indication of combustion efficiency and is composed of fuel that is not completely burned (Naima & Liazid, 2013, Enweremadu & Rutto, 2010). Hydrocarbon emissions are normally as a result of incomplete combustion. The amount of UBH emitted depend on engine operating conditions, fuel properties and air-fuel mixing in the combustion chamber (Enweremadu & Rutto, 2010). Most literature reported that the higher the concentration of TPO in a blend the higher the HC emissions of the engine. Murugan *et al.* (2008b) studied the effects of load on HC emissions of TPO-DF blends. The authors noted higher emissions at full and low loads while blends with higher TPO content resulted in higher HC emissions. The high aromatic nature of TPO could also cause an increase of unburned hydrocarbon. One study (Doğan *et al.*, 2012) reported lower HC emission for blends of up to 50% TPO with petro-diesel fuel and higher HC for blends with more than 50%. The viscosity of the oil in that work was less than that of petro-diesel fuel. JMETPO blends of 10 and 20 percent showed lower HC emissions compared to reference petro-diesel fuel due to better combustion of JME (Sharma & Murugan, 2013).

CO is a colourless and very toxic gas and its emission should be kept as low as possible. CO emissions depend on air-fuel ratio, a rich mixture tends to increase CO emission (Naima & Liazid, 2013) while at lean mixtures the CO will be further oxidised to $CO_2$. While some

authors have reported an increase in CO with increase of TPO in the blend, others have found no significant difference. İlkılıç & Aydın (2011) observed a reduction in CO emissions with increase in engine speed for both petro-diesel fuel and blends with TPO. This is due to the fact that as engine speed increases, the air movement in the cylinder creates a more uniform air-fuel mixture leading to improved combustion, and consequently lower CO emissions. Though, in general, the CO content from TPO and its blends was found to be higher than that of petro-diesel fuel (İlkılıç & Aydın, 2011). Doğan *et al.* (2012) observed a reduction in CO emissions with increase in TPO content in blends at lower speeds (1400 & 2000 rpm) while at higher speeds (2600-3200 rpm) an opposite trend was noted. However, these differences in CO emissions were not significantly different to those of petro-diesel fuel.

$NO_x$ emissions are formed by a series of reactions between nitrogen and oxygen in the air. Both TPO (Murugan *et al.*, 2008b) and DTPO (Doğan *et al.*, 2012) blends with petro-diesel fuel exhibited high $NO_x$ emissions compared to petro-diesel fuel. The effect of speed on $NO_x$ emission was studied by İlkılıç & Aydın (2011). They reported that at low and medium speeds TPO100 and blends with high concentration of TPO exhibited significantly lower $NO_x$ emissions, the opposite trend was noted at high speeds. $NO_x$ emissions are mainly affected by aromatic content, cylinder gas temperature, density and residence time (Jaichandar & Annamalai, 2013, Enweremadu & Rutto, 2010, Tan *et al.*, 2013, Hossain & Davies, 2013, Murugan *et al.*, 2008b). Fuels with high aromatic content exhibit longer ignition delay, thus, leading to increase in $NO_x$. The aromatic content of TPO is higher than that of petro-diesel fuel, therefore, it is expected that the $NO_x$ values will increase with increased TPO content in the blend.

Limited literature was found on $SO_2$ emission. An increase in $SO_2$ with use of TPO or with an increase in TPO concentration in blends was reported (İlkılıç & Aydın, 2011). In that work, it

was found that $SO_2$ increased almost linearly with TPO content in blends. This was probably due to the high sulphur content in the TPO. The Sulphur content of TPO in their work was 4.5% higher than that of petro-diesel fuel.

Smoke consists of soot in exhaust gas. Smoke opacity is essential, since it shows the amount of pollutants emitted, higher smoke may indicate higher particulate matter (İlkılıç & Aydın, 2011). It was found that TPO10 and TPO50 (Murugan *et al.*, 2008b) had similar smoke emission levels but slightly higher than that of petro-diesel fuel. This was attributed to the higher aromatic content of TPO. In a similar study, İlkılıç & Aydın (2011) found that all blends exhibited higher smoke opacity levels than that of petro-diesel fuel. The reasons given were the high density and large TPO molecules could have given rise to poor atomisation. Smoke opacity of DTPO was found to reduce with an increase in DTPO concentration in the oil (Doğan *et al.*, 2012). The low flash point and viscosity of DTPO was attributed to this observation. Low flash point for a fuel means high volatility.

In general, any factor that causes incomplete combustion will also lead to an increase in HC and CO emissions. These could include higher density, poor volatility, high aromatic content, rich fuel mixtures, lower Cetane number, longer ignition delay and higher carbon residue (İlkılıç & Aydın, 2011, Doğan *et al.*, 2012, Murugan *et al.*, 2008b). Diesel engines are designed to run on a lean mixture. The density of TPO is generally higher than that of diesel so when fuel is being injected into the combustion chamber, due to the higher density, more fuel will be injected into the chamber on mass basis leading to a rich mixture. It has been shown by (Tan *et al.*, 2013) that emissions such as exhaust smoke, PM, NOx, HC and CO reduce with a decline of fuels' aromatic content. Martínez *et al.* (2014) found the aromatic content of TPO to be 65.2%, which was much higher than that of petro-diesel fuel at 29.8%. This could also explain why the emissions of TPO are higher than that of petro-diesel fuel.

## 2.4    Diesel Engine modelling

Engine modelling is carried out for two main purposes; to predict engine performance without performing tests and to determine the parameters that cannot be evaluated experimentally (Richard, 1992). The complexity of processes in the diesel engine make it difficult to model from first principles, as a result engine models rely a lot on experimental data and empirical correlations (Richard, 1992). For example, in a turbo charged diesel engine, the following processes may be involved; air compression and intercooling, unsteady flow in the induction systems, flow through valves, spray formation and penetration, air/fuel mixtures in the combustion chamber, injection system dynamics, combustion, heat transfer, turbine performance amongst others (Richard, 1992).

Estimation of engine performance at a given speed and loads is normally done using engine performance maps which are experimentally generated (Celik & Arcaklioğlu, 2005, Richard, 1992). The maps mainly display contours of BMEP and BSFC, but can also contain plots for emissions, ignition timing and air/fuel mixture strength (Richard, 1992). These parameters are plotted graphically against speed. Generating these engine maps is a long and tedious process besides the requirement of skilled personnel and specialised instruments. For example, 400-600 engine test runs at different combination of speed and load may be required to generate a fuel consumption map for a particular engine (Rawlins, 2005).

Traditionally, the diesel engine combustion process has been simulated using mathematical models. However, these models have several limitations and assumptions. Mathematical models for diesel engine combustion can be divided into two groups; thermodynamic models and multidimensional models. Thermodynamic models can further be divided into two groups of models. Single-zone models and multi-zone models. Single zone models assume the air/fuel charge into the combustion chamber is homogenous in temperature and composition and

behaves like an ideal gas. The first law of thermodynamics is applied assuming that the working fluid is a thermodynamic system undergoing mass and energy transfer. Single zone modelling leads to a series of ordinary differential equations for charge pressure, temperature and mass. This model does not take fuel vaporisation and variation in temperature and composition into account. This assumption of homogeneity in single zone models is unrealistic. Multi-zone models take this analysis further by dividing injected liquid into different zones assumed to have even composition and temperature. Thus, accounting for the variation of turbulence, pressure, temperature and composition. These models are mainly used to predict cylinder pressure and heat release rate as a function of crank angle (Richard, 1992).

## 2.5    Artificial Neural Network

Artificial Neural Network (ANN) is a data processing system inspired by the biological central nervous system (Oğuz *et al.*, 2010, Ghobadian *et al.*, 2009). It consists of interconnected neurons that pass information to each other. The connections have weights that can be adjusted based on experience, hence making the network adopt to input and capable of learning. ANN can predict multiple outputs from multiple inputs which are variable and an input or output without prior knowledge of their relationship (Oğuz *et al.*, 2010). The predictive capability of a neural network results from training with empirical data then validation by independent data (Ghobadian *et al.*, 2009).

### 2.5.1    The neuron

The basic element of the NN is the neuron which consists of weights (w), biases (b) summers and transfer function as shown in Figure 2.2a. But usually, a neuron has more than one input as illustrated in Figure 2-2b. Three processes take place in the neuron. The first process is referred to as the weight function, where the scalar input $p$ is multiplied by scalar weight $w$ to form product $wp$. The net function weighted input $wp$ is added to the scalar bias b to form the

net input n. Finally, the net input is passed through the transfer function, which produces the scalar output a.
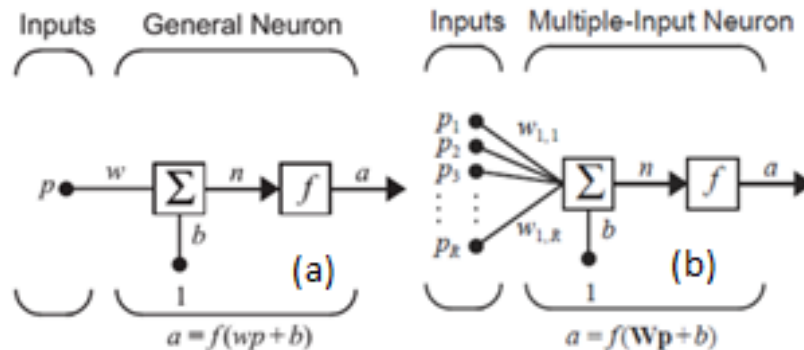


Figure 2-2 Single input (a) and multiple input (b) neuron (Demuth & Beale, 1993)

## 2.5.2 Network architectures

Two or more neurons combine to form a layer (Figure 2-3). A typical neural network consists of three layers; input, output and hidden layer(s), each consisting of a network of interconnected neurons (Oğuz *et al.*, 2010, Ghobadian *et al.*, 2009). The input layer comprises of all the input variables which are then processed in the hidden layer(s) and the output is computed in the output layer. The number of neurons in the input layer corresponds to the number of input variables while the number of neurons in the output layer correspond to the output parameters. Each neuron has a transfer function that receives signals from the neurons in the previous layer (Celik & Arcaklioğlu, 2005).
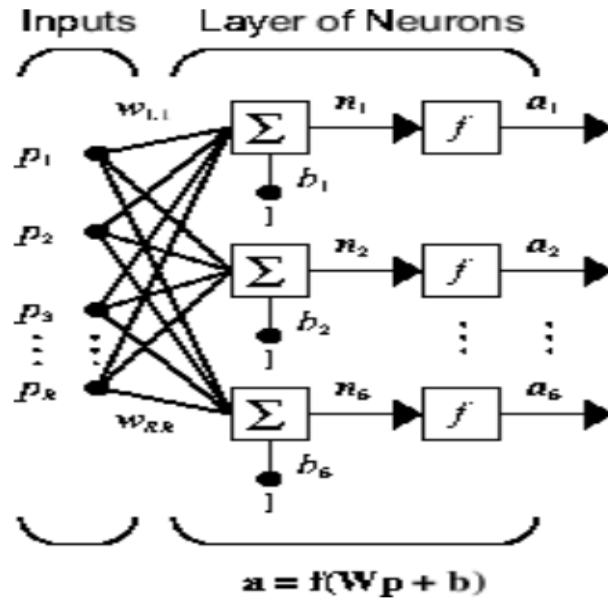
Figure 2-3 One-layer network with r input elements and r neurons (Demuth & Beale, 2001)

Each neuron receives an input $p_1, p_2, p_3 \ldots p_k$. Each input is then multiplied by the corresponding weight of the neuron connection $w_{sr}$. Where $s$ indicates destination neuron of the weight and $r$ indicates the source of the weight. The bias $b_s$ which has a non-zero value is added to the summation of inputs to give a net input $n_s$ (2-7).

$$n_S = \sum_{r=1}^{r} w_{sr} p_r + b_r \qquad\qquad 2\text{-}7$$

Finally, the net input is processed according to the type of transfer or activation function, to yield scalar output $a_s$ (2-8)

$$a_s = f(n_s) \qquad\qquad 2\text{-}8$$

The neuron layer outputs form a column vector **a,** represented by 2-9.

$$a = f(Wp + b) \qquad\qquad 2\text{-}9$$

$$w = \begin{bmatrix} w_{1,1} & w_{1,2\dots\dots} & w_{1,R} \\ w_{2,1} & w_{2,2}\ \dots & w_{2,R} \\ & & \\ w_{S,R} & w_{S,2}\ \dots & w_{S,R} \end{bmatrix} \qquad\qquad 2\text{-}10$$

A network can have several layers as shown in Figure 2-4. Each having a weight matrix (2-10) a bias vector **b,** and an output vector **a**. The outputs for each intermediate layer are the inputs for the following layers as shown by 2-11 to 2-14.
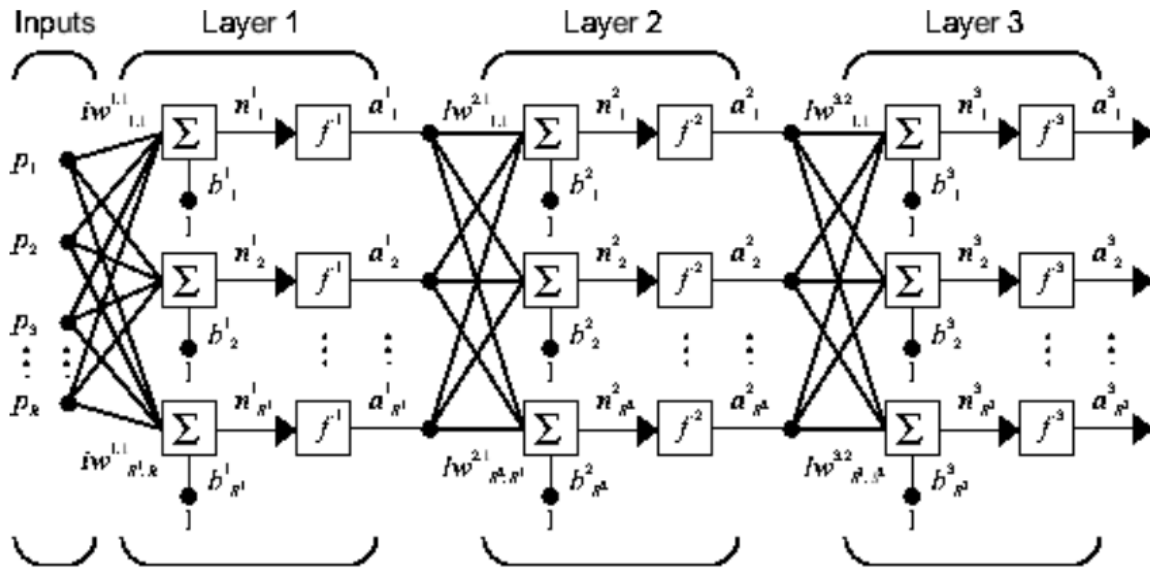


Figure 2-4 Three layer network (Demuth & Beale, 2001)

$$a^1 = f^1(IW_{1,1}p + b_1) \qquad\qquad 2\text{-}11$$

$$a^2 = f^2(LW_{2,1}p + b_2) \qquad\qquad 2\text{-}12$$

$$a^3 = f^3(LW_{3,2}p + b_3) \qquad\qquad 2\text{-}13$$

$$a^3 = f^3(LW_{3,2}f^2(LW_{2,1}f^1(IW_{1,1}p + b_1) + b_2) + b_3) \qquad 2\text{-}14$$

Weights and bias are adjustable parameters of the neuron. The idea is to be able to adjust them to exhibit a certain behaviour. The transfer function is selected by the designer and then the weights and biases will be adjusted by some learning rule in such a manner that the neuron input/output relationship meets a desired target. This process is called training. The objective of training is to get the optimum set of weights which minimises the error. Each neuron has a

transfer function that receives signals from the neurons in the previous layer (Celik & Arcaklioğlu, 2005).

### 2.5.3 Transfer function

Transfer function brings non-linearity into the neural network, making it more superior to linear transformation (Roy *et al.*, 2014). A particular transfer function is selected to meet some requirement of the problem that the neuron is trying to solve. ANN is sensitive to the nature of data, therefore, different data sets require different transfer functions (Ismail *et al.*, 2012). Linear (pureline), log sigmoid (logsig) and tangent sigmoid (tansig) are the most common transfer functions used, they normalise data to a range used by the transfer function (Ismail *et al.*, 2012). The output of a linear transfer function (Figure 2-5) is equal to its input ($a = n$). Neurons of this type are suitable for use in the final layer of multilayer networks (Yusaf *et al.*, 2011).



$$a = purelin(n)$$
Linear Transfer Function

$$a = purelin(wp + b)$$
Single-Input *purelin* Neuron
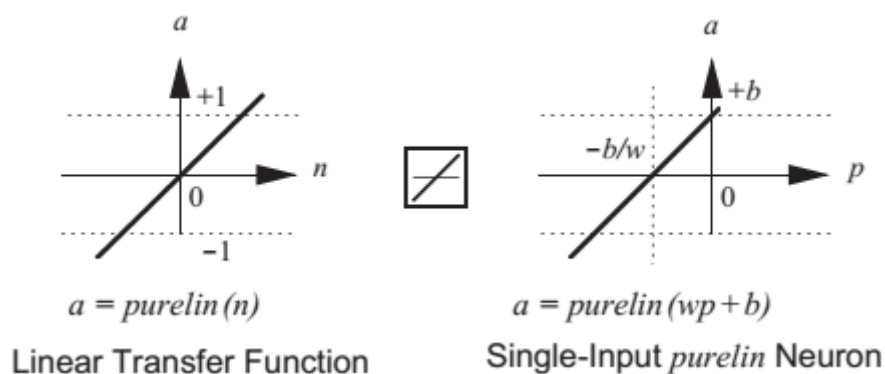
Figure 2-5 Linear transfer function (Demuth & Beale, 2001)

The log-sigmoid transfer function resets the input that may have a value of between plus and minus infinity into the range of 0 to 1 according to 2-15. The log-sigmoid transfer function (Figure 2-6) is commonly used in hidden layers of multilayer networks that are trained using the back-propagation algorithm partly because this function is differentiable (Demuth & Beale, 2001).

$$a = \frac{1}{1-e^{-n}} \qquad\qquad 2\text{-}15$$
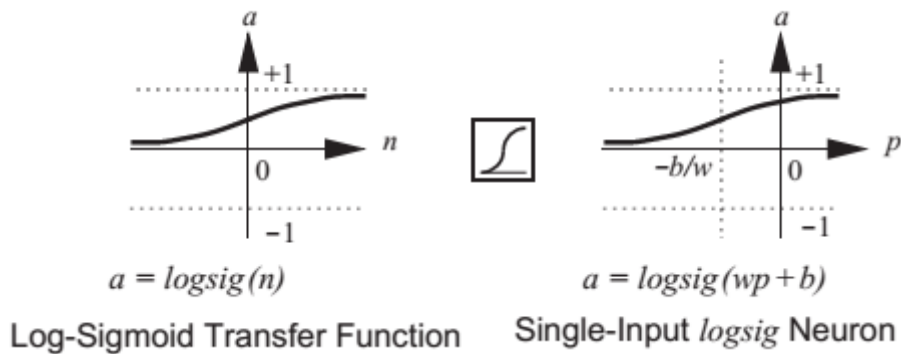


Figure 2-6 Log sigmoid transfer function (Demuth & Beale, 2001)

Other transfer functions include the hard limit, symmetrical hard limit, saturating linear, symmetrical saturating linear, Hyperbolic, Tangent Sigmoid, positive linear and competitive transfer function. More details of these transfer functions can be found in Demuth & Beale, (2001).

### 2.5.4 Neural network design process

Neural network design process primarily involves seven steps (Demuth & Beale, 2001); (i) Collect data (ii) create the network; (iii) Configure the network; (iv) Initialise the weights and biases; (v) Train the network; (vi) Validate the network; and (vii) use the network. After the data have been collected and the network created, it is configured and trained. Configuration involves setting up the network input and output sizes, preprocessing settings and initialising weights in such a manner that it is compatible with the problem and sample data. Training involves adjusting weights and biases in such a way that the network's performance is optimised. Once training is complete the networks prediction ability is analysed. If performance is satisfactory the network can be used to make new predictions.

The basic training process is as follows (Demuth & Beale, 2001, Celik & Arcaklioğlu, 2005, Ismail *et al.*, 2012): Inputs are introduced to a network together with desired output(s). Signals from input layers are conveyed to neurons in the hidden layers. The transfer function estimates the non-linear behaviour of the input data set. Weights and biases of the interconnected neurons, which were initially randomly chosen, are adjusted while targeting the desired output (Figure 2-7). This process is repeated over several iterations until a satisfactory level of performance is achieved, then training stops and the network stores this information as knowledge. The network can now be used to make predictions.
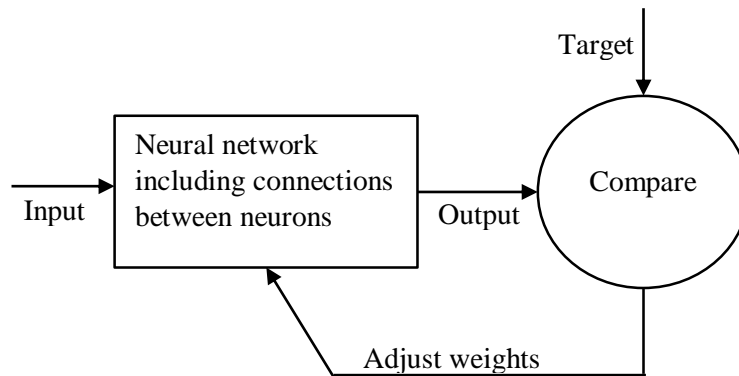


Figure 2-7 Basic neural network training process (Demuth & Beale, 2001)

### 2.5.5 Model evaluation

The objective of training a neural network is to minimise error between the output and the target values. Evaluation of the accuracy of the network is usually done with a statistical method. They include; Sum of Squares Error (SSE), Mean Square Error (MSE), Mean Absolute Percentage Error (MAPE), Root Mean Square Error (RMSE) and the correlation coefficient squared $R^2$ (Demuth & Beale, 2001). The MSE, SSE and RMSE show the difference between predicted and actual values, $R^2$ shows the proportionality of predicted and actual data sets. The $R^2$ value is always between 0 and 1. A value closer to one indicates that there is a good

correlation between predicted and experimental values. A value close to zero indicated a poor correlation. These statistical evaluation methods are defined by the equations below.

$$SSE = \left( \sum_J |t_j - o_j|^2 \right) \quad \dots\dots\dots\dots\dots\dots\dots\dots\dots\dots\dots\dots\dots\dots\dots\dots\dots\dots\dots\dots\dots \quad 2\text{-}16$$

$$MSE = \left( \left( \frac{1}{P} \right) \sum_J |t_j - o_j|^2 \right) \quad \dots\dots\dots\dots\dots\dots\dots\dots\dots\dots\dots\dots\dots\dots\dots\dots\dots \quad 2\text{-}17$$

$$RMSE = \sqrt{\left( \left( \frac{1}{P} \right) \sum_J |t_j - o_j|^2 \right)} \quad \dots\dots\dots\dots\dots\dots\dots\dots\dots\dots\dots\dots\dots\dots \quad 2\text{-}18$$

$$MAPE = \frac{1}{p} \sum_j \left( \frac{t_j - o_j}{t_j} \times 100 \right) \quad \dots\dots\dots\dots\dots\dots\dots\dots\dots\dots\dots\dots\dots\dots \quad 2\text{-}19$$

$$R^2 = 1 - \left( \frac{\sum_J (t_j - o_j)^2}{\sum_j (o_j)^2} \right) \quad \dots\dots\dots\dots\dots\dots\dots\dots\dots\dots\dots\dots\dots\dots\dots\dots \quad 2\text{-}20$$

Where t is the target value, o is the output value and p is the number of pattern.

### 2.5.6 Feed forward, back-propagation

The most popular and commonly used algorithm is the back-propagation (BP) algorithm, it consists of two stages; the feed forward and back-propagation (Oğuz *et al.*, 2010, Sharma *et al.*, 2016). Feed forward NN is a type of NN architecture where information is fed forward from the input layer through the hidden layers to the output layer (do not form connections or loops) (Taghavifar *et al.*, 2015). Back-propagation is a training algorithm that minimises error between input and output by gradient decent (Roy *et al.*, 2014). The errors between targeted and predicted values are calculated and then propagated backwards after feed forward, and the weights are adjusted with this algorithm to minimise the error (Taghavifar *et al.*, 2015). Several iterations take place, each time with a new set of weights and biases, and stops after a certain set of weights that minimises the error is arrived at (Bietresato *et al.*, 2015, Mwasiagi *et al.*, 2008). The weights are adjusted in such a manner that some inputs are made more significant

than others and will, therefore, have a larger influence when the output is calculated. Once the network is trained it can generalise to similar cases.

Due to shortcomings such as slow convergence rate, the standard Back-Propagation (BP) algorithm is not appropriate for practical problems, as a result, heuristic and numerical optimisation techniques have been developed to hasten the process (Mwasiagi *et al.*, 2008, Rao *et al.*, 2016). The heuristic techniques can be classified as variable learning rate and resilient back-propagation training algorithms. Numerical optimisation techniques can be classified as conjugate gradient, quasi-Newton or Levenberg-Marquardt algorithms (Mwasiagi *et al.*, 2008, Sharma *et al.*, 2016, Rao *et al.*, 2016).

### 2.5.7 Data requirements and preparation for neural network

Though the general perception is that a lot of data sets are required for neural network modelling, there is no information on the exact number of data sets that are adequate to train a NN. Related studies have shown that with as little as 30 data sets, ANN models can converge and make accurate predictions. Silitonga *et al.* (2015) used 30 experimental data sets to train (25 data sets for training) and test (5 data sets for testing) a ANN model to predict engine performance, emission and combustion of a turbo charged diesel engine based on engine speed and percentage fuel blend. The authors noted that the correlation coefficient was within the range of 0.9798–0.9999 for the ANN model and test data. Ilangkumaran *et al.* (2016) used 19 experimental data values for training and 11 values for testing. That is a total of 30 data sets to train and evaluate the model. In this work, the authors had two input parameters of engine load and fuel blend percentages, and the model could satisfactorily predict seven engine characteristics.

It is important to note that NN can only generalise well within the range of inputs used for training, beyond this limit it cannot accurately extrapolate (Demuth & Beale, 2001). Thus, it is

essential to have data sets which span within the limits for which the network will be used. It is also important to scale down or normalise data within a certain range e.g. -1 to 1 or 0 to 1 (Rotich, 2014) depending on the transfer function. This ensures that each input variable offers the same influence in the ANN (Rao *et al.*, 2016). Thus training becomes faster, memory efficient and it produces more precise results (Rotich, 2014, Ilangkumaran *et al.*, 2016) normalising of data also helps to improve the performance of the network (Ilangkumaran *et al.*, 2016).

## 2.6   Application of Artificial Neural Network in modelling diesel engine parameters

Due to the lengthy computations involved in mathematical and simulating programs, machine learning methods such as ANN are attractive due to their simplicity, accuracy and fast response (Ghobadian *et al.*, 2009, Mohammadhassani *et al.*, 2015). ANN is being accepted as a fast, powerful and accurate tool for prediction of relationships between engine parameters and output responses based on experimental data (Ismail *et al.*, 2012). It has been successful in predicting various aspects of the diesel engines with a high level of accuracy. Ghobadian *et al.* (2009) found that ANN was satisfactory in predicting Torque, Specific Fuel Consumption, HC and CO emissions of a diesel engine running on waste cooking oil biodiesel using the back-propagation algorithm. The prediction was done based on blend concentration and engine speed. An analysis performed showed a good relationship between independent experimental data and predicted data with a correlation coefficient close to one and a mean square error of 0.0004. In a related study, (Oğuz *et al.*, 2010) ANN was used to estimate the Brake Power, torque, fuel consumption and Specific Fuel Consumption of an engine running on blends of petro-diesel fuel, biodiesel and bioethanol. A statistical t-test analysis between the predicted and experimental results showed no significant difference at 95% reliability. Nikzadfar & Shamekhi (2014) employed ANN to investigate the contributive effect of 10 operational

parameters on the performance of a common rail diesel engine. A 6% error was noted between predicted and experimental results. These parameters include; inlet pressure and temperature of air, mass of injected fuel, exhaust gas recirculation rate, exhaust gas temperature, injection timing on torque, soot $NO_x$ and Brake Specific Fuel Consumption. Spray quality as a function of engine variant parameters has been investigated using the Levenburge-Marquardt training Algorithm of ANN by Taghavifar *et al.* (2014). The spray quality parameters; sauter mean diameter and penetration were predicted with $R^2$ values closer to 1. These parameters were predicted with respect to crank angle, vapour mass, flow rate, turbulence and nozzle outlet pressure. ANN has been used for engine diagnosis of the diesel engine. Diagnosing of misfiring of one or more cylinders is usually done by measuring cylinder pressure, this requires the installation of a pressure sensor which is a taxing process. Jianmin *et al.* (2011) used the back-propagation algorithm to diagnose the diesel engine misfire. ANN was able to accurately locate a misfiring cylinder based on cylinder vibration signal. From data of exhaust gas temperature and engine speed Bietresato *et al.* (2015), was able to estimate torque and BSFC of a farm tractor engine using ANN. However, the results showed that the prediction of torque was more accurate than that of BSFC. Rawlins (2005) developed an ANN model to aid in monitoring the performance of the diesel engine operation in industrial set up. Roy *et al.* (2014) was able to predict BSFC, BTE, CO2, NOx and PM with regard to load, fuel injection pressure, EGR and fuel injected per cycle. The ANN model showed results which showed excellent correlation with empirical data, where the mean square error was within the range of 1.1 and 4.57%, and correlation coefficients within the range of 0.987–0.999. Mohammadhassani *et al.* (2015) successfully employed the combination of artificial neural network (ANN) and Ant colony optimisation (ACO) algorithm for modelling and reducing NOx and soot emissions from a direct injection diesel engine. The combination of ANN and ACO yielded a 32% and 7% reduction in $NO_x$ and soot respectively with a response time of 4 minutes. The input factors

were engine speed, air intake pressure, mass fuel injection rate and power. In view of these advances, there is evidence that ANN is a suitable tool to simulate parameters of a diesel engine satisfactorily. Ismail *et al.* (2012) noted that "ANN is now highly regarded as a promising tool in predicting accurately the complex interactions between engine control parameters and output responses rapidly".

## 2.7 Conclusion

The main products of tyre pyrolysis are liquid oil, gas and char. Given that the oil yield can go up to 65%, pyrolysis presents an alternative and suitable way of tyre disposal, especially in developing countries where there are large stockpiles of tyres like in South Africa. The quantity and quality of tyre pyrolysis products depend on reactor type, tyre particle size, heating rate and pyrolysis temperature, as opposed to tyre composition. The optimum oil yields can be obtained in temperatures ranging between 450 °C – 550 °C depending on reactor design and operating conditions. Beyond this optimum temperature, the gas yield increased because the oil and char was being volatised to gas. At lower temperatures, the solid yield was high because the temperatures are not sufficiently high enough to thermally degrade it to gas and oil. The use of a catalyst has a remarkable effect on yield.

From the reviewed literature, it can be established that pyrolysis of used scrap tyres can be used as an alternative method of disposing of waste tyres as well as producing fuel that can produce acceptable performance when in diesel engines, but only when blended in small quantities with petro-diesel fuel or with further processing.

The liquid from pyrolysis can be used for many purposes including fuel for the internal combustion engine after some modification like Sulphur reduction or blending with petro-diesel fuel or other fuels. The diesel engine is optimised for petro-diesel fuel. Thus, for any other fuel to run in the diesel engine, its properties must be as close as possible to those of

petro-diesel fuel. The properties of TPO have a significant effect on engine performance and emissions. Due to this, TPO is not suitable for use in the diesel engine in raw state or without modifications to the engine. These properties include high aromatic content, density, viscosity, sulphur content, low cetane number and most importantly, different boiling range compared to petro-diesel fuel. There is a correlation between fuel properties and boiling range of a fuel.

Literature review indicates that TPO can easily be separated into distinctive fractions based on their boiling point and be suitable for specific applications, just like crude oil. The easiest way to bring TPO closer to petro-diesel fuel is to distil TPO and extract the fraction that resembles petro-diesel fuel based on boiling range. In spite of the extensive research on TPO as fuel for the diesel engine, no literature could be found in which TPO was distilled to the fraction that resembles petro-diesel fuel and tested as fuel for the diesel engine. It may be interesting to establish the engine performance characteristics when it runs on this fuel type and its blend with petro-diesel fuel and biodiesel fuel.

Testing the diesel engine under different operating conditions is a time consuming and expensive process that also requires the use of specialised equipment which may not be easily available. After experimental evaluation of engine performance on this fuel, it may be necessary to develop a predictive model for engine performance. Modelling provides a way of simulating and understanding the engines response to different input parameters and conditions. ANN has proved to be an adequate tool for modelling and analysing engine performance. After experimental evaluation, it may be necessary to develop a predictive model that can accurately relate input parameters to engine performance when the engine is running on TPO petro-diesel fuel blends.

# 3 METHODOLOGY

## 3.1 Distillation process of tyre pyrolysis oil

The distillation apparatus for this work is shown in Figure 3.1. It consists of a 500 ml round bottomed flask connected to a 400 mm Liebig condenser packed with steel and this acted as a fractionating column. It was then connected to a condenser with water as the cooling medium. The condenser empties the condensate into a beaker. The heating mantle is rated at 400 kW and has a knob to conveniently adjust heating rate up to a maximum temperature of 400 °C. A glass thermometer with a range of -10 to 400 °C was used to monitor the temperature, with adjustment of the heat of the heating mantle.

The TPO was separated into three fractions as follows: The low boiling point fraction with a temperature range of ≤150C°, the middle distillate whose temperature range is between 150 °C and 360 °C and the heavy residue that distil at temperatures above 360 °C. The temperature of TPO was raised and maintained at 150 °C. The vapour was collected and condensed for a certain period until no more droplets were seen. The temperature was then raised to 360 °C and held there as the condensed vapour was collected in a separate container. This was continued until there was no more liquid being collected. The three fractions were stored in separate containers.

## 3.2 Characterisation of distilled tyre pyrolysis oil

Blends of DTPO with diesel fuel were prepared and are referred to as DTPO X, where X represents the percentage DTPO in the blend by mass. The blends were prepared on mass basis, because unlike volume blends, the mass fractions of each fuel in the blend remain the same with change in temperature. The fuel samples were characterised by standard methods which are shown later in Table 4-1. SANS-342 requirements for automotive diesel, properties of crude

45

TPO, and conventional diesel have also been presented in the same table for comparison purposes. The variation of temperature with density and viscosity of the oil samples was also studied. Additionally, mixing rule equations for predicting viscosity and density for both pure and blends of the oil as a function of temperature were developed and evaluated.

## 3.3 Engine performance tests for fuel samples

These tests were performed at the thermodynamics lab at the Vaal University of Technology using a set of Test Set (TD 302) complete with its auxiliaries. The parameters of interest in this work were BSFC, BTE, power, torque, emissions and combustion characteristics. The major components of the test set are shown in

Figure *3-1*

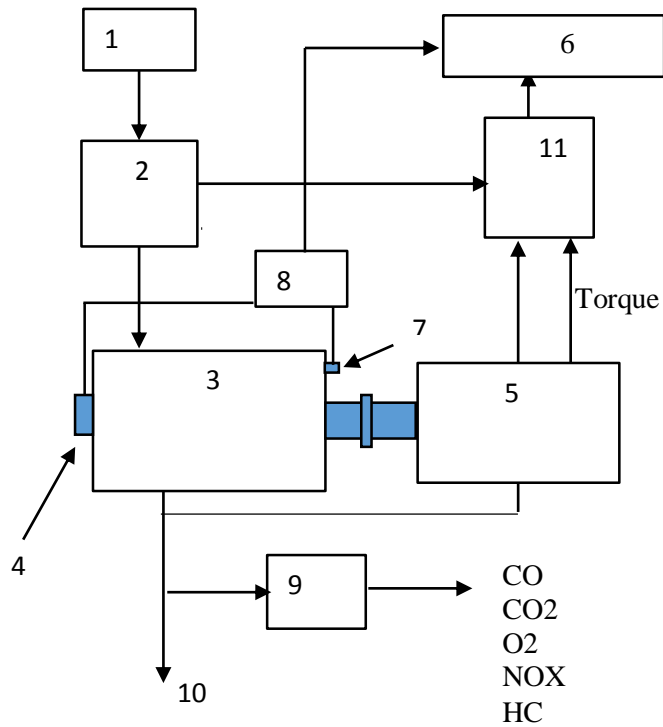Figure 3-1 A schematic layout of the engine test experiment setup

Description

1. Fuel tank

2. Automatic volumetric fuel gauge with digital readout (mm/min)

3. Diesel engine (specifications shown in Table 3.1)

4. Crank angle encoder

5. Electric Dynamometer

6. Computer

7. piezoelectric pressure transducer

8. engine cycle analyser

9. Exhaust gas Analyser (Specifications are shown in Table 3-2)

10. Exhaust

11. Versatile data acquisition system (VDAS)

Table 3-1 Engine specifications of TD302 Four-stroke Diesel engine

| | |
|---|---|
| Absolute maximum power (ISO 3046-1) | 7.3 kW (9.9hp) at 3600 rev/min |
| Continuous rated power (ISO 3046-1) | 6.5 kW (8.8 hp) at 3600 rev/min |
| Number of cylinders | 1 |
| Bore | 88 mm |
| Stroke/crank radius | 79 mm/38 mm |
| Connecting rod length | 124 mm |
| Engine capacity | 462 cm$^3$, 462 cc or 0.462 L |
| Compression ratio | 20.5:1 |
| Oil type | Multigrade SAE 10W-30 |

Table 3-2 Exhaust gas analyser specifications

| Gas | Range | Tolerance |
|---|---|---|
| Oxygen | 0 – 25% | ± 0.21 |
| Carbon dioxide $CO_2$ | 0 - 20 % | ± 0.2 |
| Hydrocarbon HC | 0 – 100% | ± 1 |
| Nitric oxide $NO_x$ | 0 – 5000 ppm | ± 50 |
| Sulphur dioxide $SO_2$ | 0 – 5000 ppm | ± 50 |
| Excess air/lambda | 0 - 99% | |

The engine speed was adjusted to 800, 1200, 1600, 2000, 2400 2800, 3200 and 3500 rev/s. At

each speed the torque, fuel flow rate, emissions, pressure/volume vs crank angle and exhaust

gas temperature were recorded. Then other parameters such as power BSFC, rate of heat rise and thermal efficiency were calculated. Before the tests began, the engine was adequately warmed up with petro-diesel fuel. The fuel lines were then drained off at each change of fuel sample.  The test fuel was run through the system for a specific duration to purge the system of any remaining fuel from the previous tests. Each test was repeated twice to ensure repeatability was within acceptable limits and average values were noted. The parameters computed were plotted in graphs against speed and a performance analysis of their performance carried out. Petro-diesel fuel was used as the baseline sample for comparison purposed.

## 3.4  Artificial neural network modelling of engine performance

The data collected in section 3.3 was used to train and validate a neural network. During this stage, four sub-problems were addressed when developing a NN.

- Description of the input parameters that adequately describe diesel engine performance which in this case will be engine speed and fuel blend ratio.
- Collection, selection and partitioning of data which best describe the problem
- Neural network topology selection, training and validation
- comparison of model output with experimental data

Selection of optimal network topology is the most important aspect in NN modelling, i.e. number of hidden layers, neurons and activation function (Omidvarborna *et al.*, 2016, Roy *et al.*, 2014, Rao *et al.*, 2016). The ANN model was developed on MATLAB 2009a platform. Training parameters are presented in Table 3-3 . MATLAB was a natural choice, because it has been extensively used by other researchers in similar studies (Omidvarborna *et al.*, 2016, Roy *et al.*, 2014, Tosun *et al.*, 2016) and due to its availability. A three-layer network; input,

one hidden and output layer were used in this work. The feed forward back-propagation architect was used for modelling.

Table 3-3 Training parameters of the proposed ANN model on MATLAB 2009a platform

| SOFTWARE | MATLAB 2009a |
|---|---|
| Training algorithm | Levenberg-Marquardt algorithm |
| Data | Training subset 70% |
| | Validation subset 15% |
| | Test Subset 15% |
| Hidden layer activation function | logsig |
| Output layer activation function | purelin |
| Performance function | Minimum MSE (1x $10^{-5}$) |
| Normalising range | 0 to -1 |

Two independent models were developed for engine performance and emissions respectively. Both models had two input variables namely engine speed and DTPO percentage concentration in the DTPO petro-diesel fuel blend. For the first model on engine performance, there were four outputs which included power, torque, BSFC and Peak pressure. Therefore, the network had two input nodes and four output nodes. The second model had three output nodes corresponding to HC, CO and $NO_x$. Data obtained from experiments were used to train the network.

In this work, 38 experimental data sets were used for training and testing. 70% was randomly selected for training, 15% for testing and 15% for validation. This was the default setting of the software, nevertheless, other researchers have used this partitioning ratio with satisfactory results (Roy *et al.*, 2014, Omidvarborna *et al.*, 2016).

The data were pre-processed and scaled to a range of $0 - 1$ according to equation

3-13-1 and in compliance with logsig transfer function.

$$X_n = \frac{X_r - X_{r,min}}{X_{r,max} - X_{r,min}} * (X_h - X_l) + X_l \qquad \text{3-1}$$

Where $X_n$ is the normalised variable input, $X_r$ raw input variable, $X_{r,min}$ and $X_{r,max}$ are maximum and minimum of input variable, and $X_h$ and $X_l$ are set to 0 and 1.

The activation functions and training and learning algorithms selected play significant roles in the network modelling (Mohammadhassani *et al.*, 2015, Ghobadian *et al.*, 2009, Sharma *et al.*, 2016). The feed forward back-propagation neural networks with a Levenberg-Marquardt training algorithm is popular and has been successfully used to make accurate estimates (Ghobadian *et al.*, 2009, Omidvarborna *et al.*, 2016, Taghavifar *et al.*, 2015, Sharma *et al.*, 2016, Rao *et al.*, 2016, Tosun *et al.*, 2016). So Levenberg-Marquardt was chosen as the training algorithm for this study. The purelin transfer function was used in the output layer while the logsig transfer functions were used in the hidden layer. This is a frequently used arrangement of activation functions in ANN modeling and has produced satisfactory results elsewhere (Sharma *et al.*, 2016, Tosun *et al.*, 2016). There are no general criteria for deciding the number of neurons in the hidden layer, it's done by trial and error (Oğuz *et al.*, 2010, Uzun, 2012, Rao *et al.*, 2016). Networks are very sensitive to the number of neurons, too many neurons in the hidden layer can lead to overfitting while too few neurons can lead to under fitting (Demuth & Beale, 2001). A suitable number of neurons used in other related studies has been found to range from 10 to 25 (Ismail *et al.*, 2012). Therefore, in this work the number of neurons was adjusted in steps of two within the same range till the highest correlation coefficient was achieved. The goal was to maximise correlation coefficient. The maximum number of epochs was set at 1000 and the correlation coefficient was selected as the function to be maximised.

The training data set was presented to the network and used for training, the gradient was computed and weights and biases adjusted according to its error (Omidvarborna *et al.*, 2016). During the training process, the error on the validation set was monitored and training stopped when generalisation stopped improving. The network weights and biases were saved at the

minimum of the validation set error. The test data were used to independently check the overall performance of the network. Finally, to evaluate the model prediction ability, a regression analysis of the network's output values and the desired target values was performed to investigate the networks generalisation. The result and findings are presented in Sections 4.3 and 4.4.

# 4    RESULTS AND DISCUSSION

The evaluated physical and chemical properties of the fuel samples are presented in Table 4-1.

## 4.1    Characterisation of oils

Table 4-1 Properties of pure fuel samples

| PROPERTY | Method/instrument | SANS 342 limits | Petro-diesel fuel | TPO | DTPO |
|---|---|---|---|---|---|
| Heating value (MJ/kg) | CAL 2K ECO calorimeter | NA | 46.0 | 43.44 | 43.7 |
| Density @ 20°C  kg/m$^3$ | SVM 3000 Stabinger | 800 | 826 | 905 | 904 |
| Viscosity @ 40 °C mm$^2$/s | Viscometer | 2.2 - 5.3 | 2.21 | 3.13 | 2.74 |
| Cetane number | ISO 5165 | 45 | 50.5 | 52.5 | 50 |
| Cloud point °C | D5773 | | -0.1 | 9.7 | -3.81 |
| Flash point °C | ISO 3679 | 55 °C min | 69.1 | <30.1 | 34.1 |
| Sulphur ppm | XRF | 500 | 245 | 14775 | 19180 |
| Copper strip corrosion | ISO 2160 | 1 max | 1a | 1b | 1b |
| Water content ppm | 200 | | 2.97 | 157 | 93.66 |
| Sulphated ash Content, % | ISO 3987 | | 0.042 | 0.016 | 0.064 |
| Total contamination mg/kg | EN 12662 | 24 MAX | 0.07 | 0.2 | 0.1 |

### 4.1.1    Viscosity of fuel samples

Viscosity of a fuel affects the quality of spray, air/fuel mixing and distribution of fuel droplets in the engine, thus, it determines the quality of combustion in the cylinder. To improve atomisation quality, viscosity is the first property to be reduced.  The standard SANS 342 recommends optimum viscosity range of 2.2 mm$^2$/s to 5.3 mm$^2$/s at 40 °C. From Table 4-1 it can be seen that distilling TPO leads to a drop in viscosity from 3.13 mm$^2$/s to 2.74 mm$^2$/s. This value is much closer to that of petro-diesel fuel at 2.21 mm$^2$/s and well within the SANS 342 specification. All the other fuels, both pure and blends met this standard specification as

seen in Figure 4-1. Figure 4-1 also shows the effect of temperature on viscosity of the various
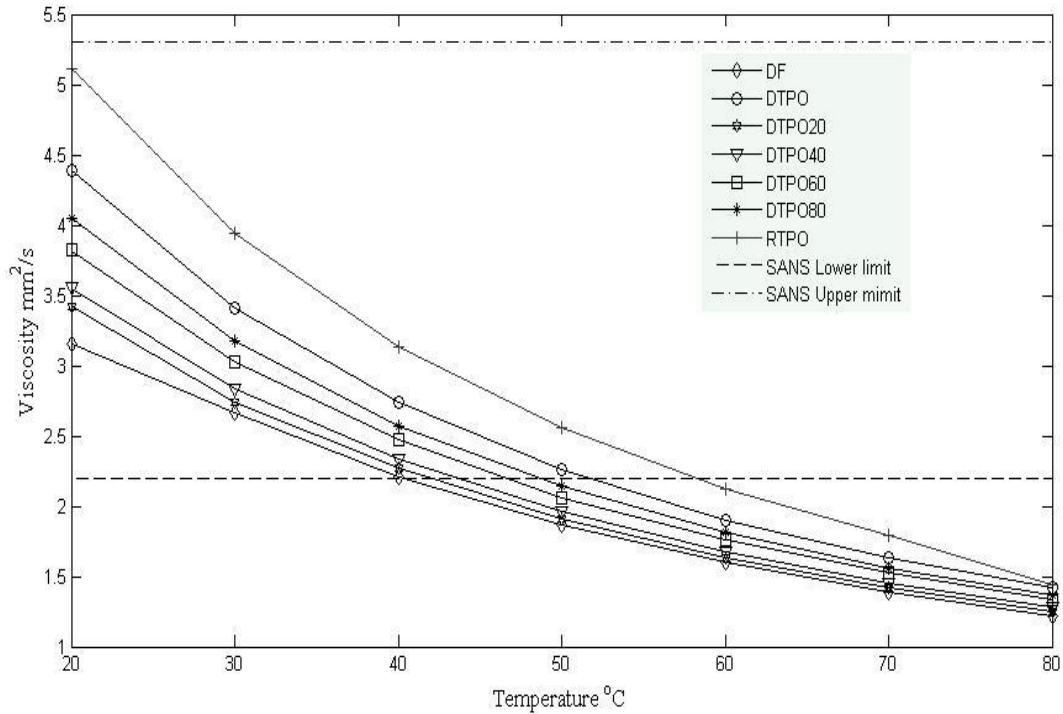
fuel samples.



Figure 4-1 Variation of viscosity of the fuels with increase in temperature

It can be seen that the temperature dependent behaviour for all the samples is similar, there was

a reduction in viscosity with increase in temperature. As expected, the viscosity of DF/DTPO

blends increased with increase in DTPO content in the blend. Viscosity of DTPO20 and

DTPO40 were very close to that of petro-diesel fuel. Unlike other properties the relationship

between viscosity and temperature/blend concentration does not follow a linear trend since it

depends on molecular interactions (Centeno *et al.*, 2011). The experimental data in Figure 4-1

was correlated by second degree Equation (4-1) as a function of temperature, where A, B and

C are constants and are presented in Table 2. $\eta$ is viscosity and T represents temperature. In

addition, Andrade-type Equation 4-S2, which is commonly used to express the variation of

temperature with viscosity, was also used to make estimates and its coefficients are also presented in Table 4-2. Absolute Percentage Deviation (APD) given in Equation 4-3 is commonly used to evaluate the suitability of these equations in making estimates (Selim *et al.*, 2015). Where $\varphi_{exp}$ is the experimental value and $\varphi_{pr}$ is the predicted value. Table 4-3 shows the measures and calculated viscosity using both Equations 4-1 and 4-2. APD is also presented in the same table. From Table 4-3 the lowest APD, when using Equation 1, is -1.79 while the highest is - 6.55. But when using Equation 4-2, the APD vary over a narrower range of -2.9 to -3.9%. Thus from the results, Equation 4-2 is better at making estimates for viscosity than Equation 1 since the values of APD obtained by Equation 4-2 vary within a narrower range than for Equation 4-1.

$$\eta = AT^2 + BT + C \tag{4-1}$$

$$ln\,\eta = A + \frac{B}{T} + \frac{C}{T^2} \tag{4-2}$$

$$APD = \frac{\varphi_{exp} - \varphi_{pr}}{\varphi_{exp}} \tag{4-3}$$

Table 4-2 Regression parameters for Equations 1 and 2

| Fuel type | Equation 1 Coefficients | | | Equation 2 Coefficients | | |
|---|---|---|---|---|---|---|
| | A | B | C | A | B | C |
| DTPO | 0.0005 | -0.101 | 6.0588 | -0.7713 | 100.5297 | -1112 |
| DTPO80 | 0.0005 | -0.09 | 5.5416 | -0.7701 | 96.9717 | -1073.5 |
| DTPO60 | 0.0004 | -0.084 | 5.2211 | -0.7004 | 89.9115 | -983.1 |
| DTPO40 | 0.0004 | -0.075 | 4.8125 | -0.7684 | 91.41 | -1015 |
| DTPO20 | 0.0004 | -0.071 | 4.6191 | -0.76 | 89.2956 | -991.389 |

Table 4-3 Measured and estimated values of viscosity for Equation 4-1 and 4-2 along with APD

| Fuel type | $\varphi_{EXP}$ | Equation 1 | | Equation 2 | |
|---|---|---|---|---|---|
| | | $\varphi_{PR}$ | APD | $\varphi_{PR}$ | APD |
| DTPO | 2.7417 | 2.8268 | -3.10391 | 2.848927 | -3.91097 |
| DTPO80 | 2.573 | 2.7416 | -6.55266 | 2.673143 | -3.89208 |
| DTPO60 | 2.4689 | 2.5131 | -1.79027 | 2.541997 | -2.96073 |
| DTPO40 | 2.334 | 2.4485 | -4.90574 | 2.416874 | -3.55073 |
| DTPO20 | 2.2765 | 2.4111 | -5.91259 | 2.346142 | -3.05916 |

### 4.1.2 Density fuel samples

SANS 342:2006 only sets a minimum limit of density for the fuel at 800 kg/m$^3$. The upper limit is not set. From Figure 4-2, the density of all the fuel samples and their blends are well above this limit and higher than that of petro-diesel fuel. From Table 4-1, there was no difference in the densities of TPO (904 kg/m$^3$) and DTPO (905 kg/ m$^3$). Therefore, the distillation process did not affect density. The density of the fuel is a very important parameter. Since fuel is metered to the diesel engine on volume basis, a fuel of high density has more mass per unit volume than a fuel of low density. Therefore, a fuel with high density is likely to produce more engine power than a fuel with low density. However, this could also be a problem when the fuel density is very high. It can lead to a rich air/fuel mixture resulting in incomplete combustion and an increase in HC, CO and soot can occur (İlkılıç & Aydın, 2011). Other authors have observed an increase in NO$_x$ emission with increase in density (Hossain & Davies, 2013, Doğan et al., 2012). The effect of temperature on density is shown Figure 4-2. It can be seen that density reduces linearly with increase in temperature. Experimental data were correlated by linear regressions as shown in Equation 4-4, where ρ is density, A and B are

constants and T is temperature. From Table 4 it can be seen that the equation fits the data well with regression coefficient ($R^2$) higher than 0.99, so there was no need for higher degree equations. The values for constants A and B are presented in Table 4-4.
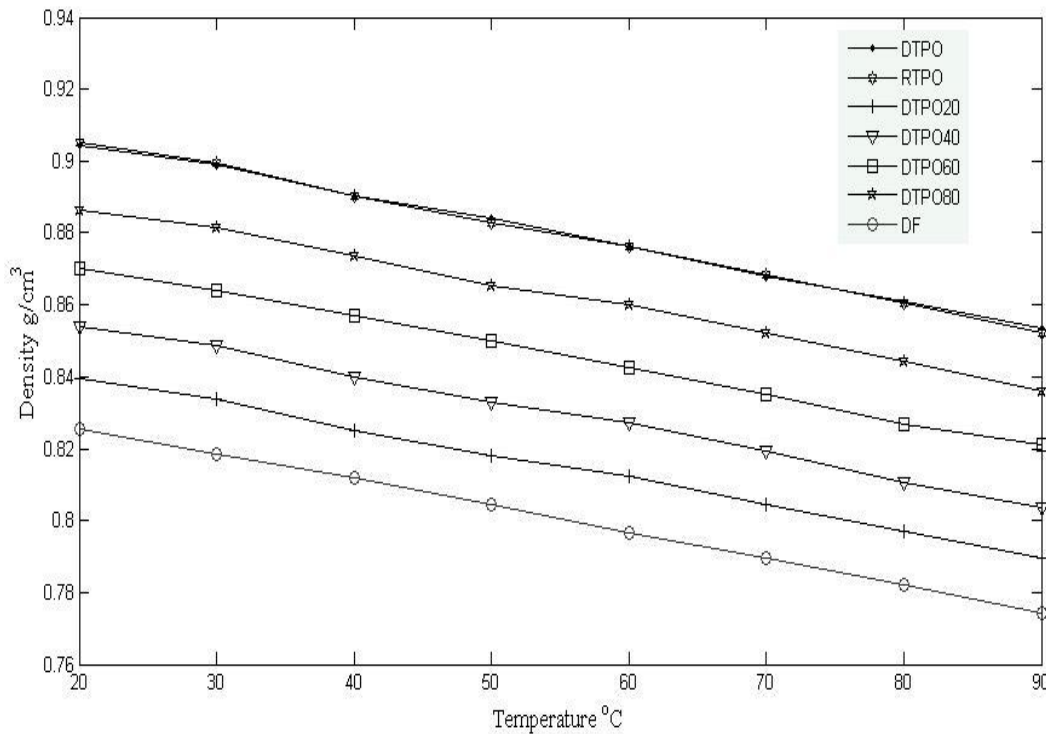
$$\rho = At + B \qquad\qquad\qquad 4\text{-}4$$



Figure 4-2 Variation of density of the fuels with temperature

The variation of density and viscosity with DTPO blend concentration is shown Figure 4-3. The density was measured at 20 °C while the viscosity was measured at 40 °C. Both density and viscosity increased with DTPO percentage in the blend. The density increased from 0.826 kg/m$^3$ for pure petro-diesel fuel to 0.904 kg/m$^3$ for pure DTPO. The viscosity increased from 2.21 mm$^2$/s for pure petro-diesel fuel to 2.74 mm$^2$/s for pure DTPO. The heating value of petro-diesel fuel was 46 MJ/kg while that of DTPO was 43.7 MJ/kg. The density, viscosity and heating value of TPO was 0.905 kg/m$^3$, 3.13 mm$^2$/s and 43.44 MJ/kg respectively as can be seen in Table 4-1. Distilling TPO reduced viscosity significantly while the difference in heating

value and Density was not significant. The sulphur content also reduced by 22 %, from 19,180 to 14,775 ppm.
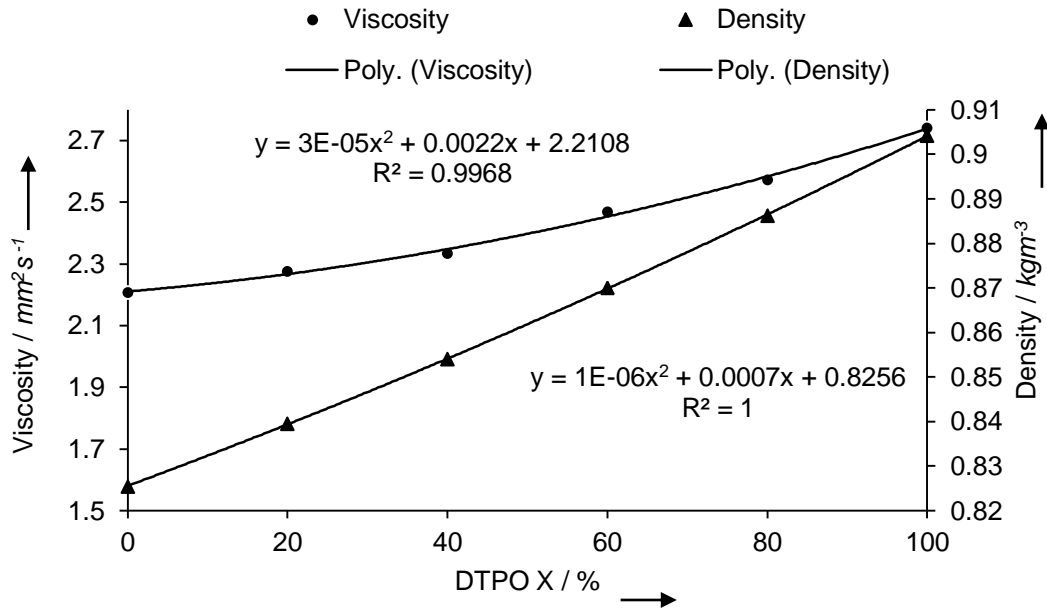


The graph shows viscosity and density data. Equations shown:
$$y = 3E{-}05x^2 + 0.0022x + 2.2108$$
$$R^2 = 0.9968$$
$$y = 1E{-}06x^2 + 0.0007x + 0.8256$$
$$R^2 = 1$$

Figure 4-3 Variation of density and viscosity with blend concentration

Table 4-4 Linear regression parameters for fuel densities

| Fuel | A | B | $R^2$ |
|------|-----|-----|-------|
| DTPO | -0.0007 | 0.9203 | 0.9986 |
| DTPO80 | -0.0007 | 0.9026 | 0.9976 |
| DTPO60 | -0.0007 | 0.8856 | 0.9986 |
| DTPO40 | -0.0007 | 0.8698 | 0.9983 |
| DTPO20 | -0.0007 | 0.8548 | 0.9989 |
| DF | -0.0007 | 0.8406 | 0.9998 |

### 4.1.3    Heating value fuel samples

The most important property of a fuel is the amount of energy produced during combusting. It shows the amount of heat released per unit mass of fuel burned and it influences power and fuel consumption of the engine. Assuming other factors to be constant, power output will tend to be proportional to heating value. From Table 4-1. The heating value of DTPO (43.7 MJ/kg) was slightly higher than that of TPO (43.44), but lower than that of DF (46.0MJ/kg). Since injector systems deliver fuel to the combustion chamber on volume basis, heating value on volume basis is a more important parameter to determine fuel consumption (Martínez *et al.*, 2013). Thus, on volume basis the heating value of DF, TPO and DTPO will be 37.997MJ/L, 39.31 MJ/L and 39.50 MJ/l respectively. Thus, of the three fuels, DTPO is expected to produce higher power, based on heating value only.

### 4.1.4    Sulphur content of fuel samples

TPO had a sulphur content of 19180 ppm but this reduced to 14755 ppm after distillation. Both samples had higher sulphur content than the recommended SANS limit of 500ppm and this could pose a problem. The sulphur content of a fuel has a significant effect on fuel emissions. It has been reported that (Tan *et al.*, 2013) exhaust smoke, HC, CO and $SO_2$ emissions reduced with reduction in sulphur content in the fuel, whereas, there was a remarkable decrease in PM emission. The authors explained that during combustion, sulphur is converted to $SO_2$, thus, consuming part of the oxygen that could have otherwise oxidised CO and HC to $CO_2$ and $H_2O$. Sulphur reaction also leads to the formation of sulphates causing accumulation of carbon, hence, soot formation. Apart from emissions concerns, sulphur can cause engine corrosion when exposed to high temperatures (Khan & Ali, 2013). For these reasons, sulphur levels should be as low as possible, hence, SANS 342:2006 recommends a maximum value of 500 ppm. Sulphur in TPO comes from the original feedstock. It is normally used as an additive to

strengthen rubber in a process known as vulcanisation. It has been estimated that after pyrolysis, about 77% of the sulphur mass in the tyre remains in the solid fraction while the remainder remains in the liquid fraction (Frigo *et al.*, 2014). The reduction of sulphur content by 22.7% after distillation is remarkable, even though it was still outside of the SANS requirements. The drop in sulphur content was because a light naphtha fraction (IBP < 160) of TPO has a high concentration of sulphur (Roy *et al.*, 1995, Benallal *et al.*, 1995) and most of this fraction was removed during distillation.

### 4.1.5   Flash point of fuel samples

This property is important with regard to safety, storage and handling of the fuel, but has no effect on engine performances. SANS has set this limit at 55 $^{o}$C. The flash point for petro-diesel fuel was 69.1 $^{o}$C, well within this limit. The flash point of DTPO (34.1 $^{o}$C) was higher than that of TPO (<30.1 $^{o}$C) even though both were lower than the recommended limit.

### 4.1.6   Copper strip corrosion of fuel samples

This test shows the potential of the fuel to corrode metal parts. Both DTPO and TPO recorded 1b while petro-diesel fuel recorded 1a, all these fuels were within the limits for SANS of 1 max. That means that they do not have the tendency to cause corrosion.

### 4.2   Engine performance emission and combustion

In this section, the effects of using DTPO as an additive to petro-diesel fuel on the engine performance, combustion and emissions are discussed. The engine was initially run on petro-diesel fuel to generate reference data. Blends were prepared containing 20, 40, 60 and 80% DTPO by mass and tests were conducted at engines speeds of 800, 1200, 1600, 2000, 2400, 2800, 3200 and 3500 rpm. These results are illustrated in Figure 4-4 to Figure *4-11* and

subsequently, a comparative analysis was performed with conventional petro-diesel fuel as the reference. The engine could run without any problems with blends of up to 60% DTPO. However, at 80% DTPO the engine became erratic, especially at high speeds. The engine speed was fluctuating and this definitely affected all other parameters. So, no further tests were performed with blends containing 80% DTPO or more.

### 4.2.1  Effects of DTPO/Petro-diesel fuel blends on engine performance

The power output of the engine and torque for DTPO/Petro-diesel fuel blends are presented and compared with the reference petro-diesel fuel in Figure 4-4 and Figure *4-5*. Engine Power is a function of torque output and engine speed. So, as expected, the graph of engine torque output verses speed and that of power vs speed showed similar characteristics. Both the power and torque increased with speed, up to a maximum point then started reducing. The maximum power and torque were noted at speeds of about 3000 rpm and 2200 rpm respectively. At low engine speeds, there is low turbulence in the cylinder leading to poor air/fuel mixing. Therefore, the combustion efficiency is low, but this will increase as speed increases, thus, leading to increased power and torque. However, as speed increases further, the volumetric efficiency of the engine decreases, leading to a reduction in power and torque output (Aydın & İlkılıç, 2015). From Figure 4-4, there was no significant difference in power for the test fuels up to a speed of 2800 rpm. Beyond this speed, the power developed by the engine reduced with an increase in DTPO concentration in the blends.  At 3200 rpm, the power developed by DTPO20, DTPO40 and DTPO60 were 2.8%, 3.0% and 5.3% respectively lower, compared to that of petro-diesel fuel. Similarly, it can be seen in Figure 4-5 that there was no significant difference in torque up to a speed of 2400 rpm. However, at 3200 rpm and 3500 rpm the torque output decreased with increase in speed. For example, at 3500 rpm, the torque for DTPO20, DTPO40 and DTPO60 was lower than that of petro-diesel fuel by 2.7%, 2.9% and 5.1% respectively. This behaviour may be attributed to the high viscosity of DTPO. At high engine speeds, there

is insufficient time for DTPO blends to vaporise, mix with air and burn efficiently as compared to the low viscosity petro-diesel fuel.
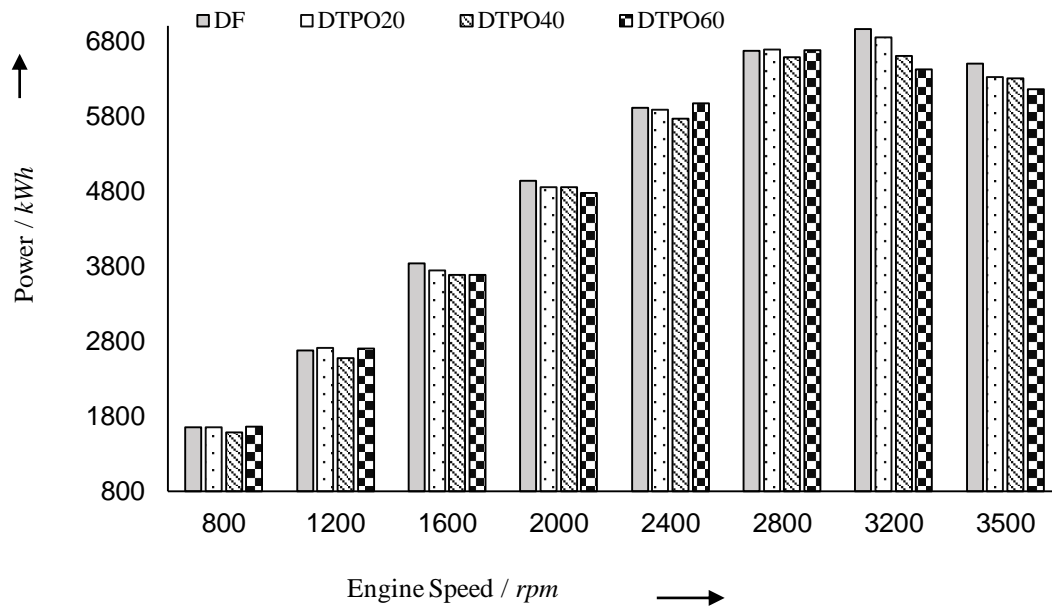


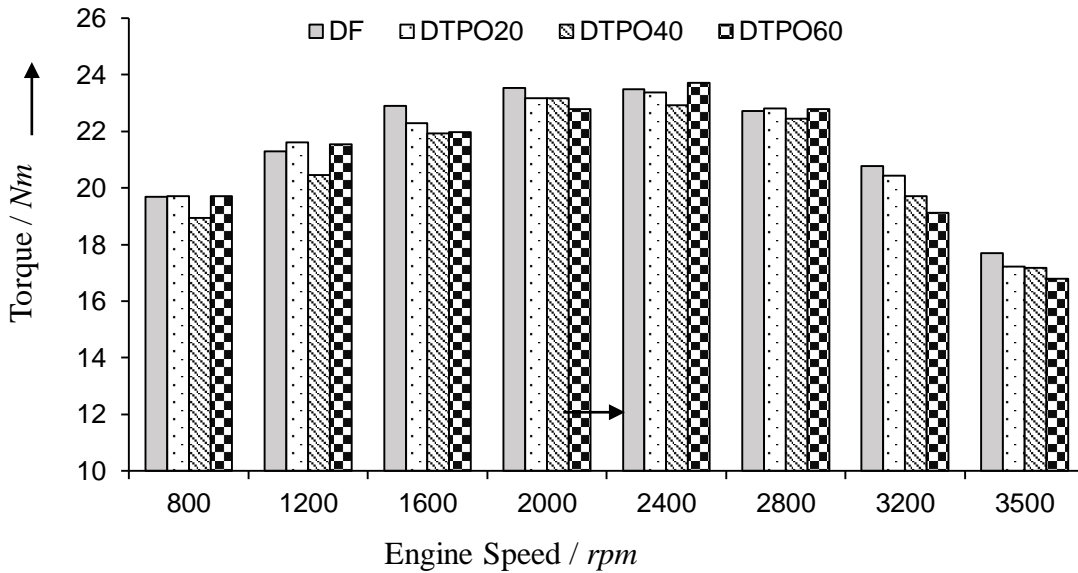Figure 4-4 Variation of power with engine speed



Figure 4-5 Variation of torque with engine speed

The changes in Brake Specific Energy Consumption (BSEC) of petro-diesel fuel and DTPO/Petro-diesel fuel blends with engine speed is illustrated in Figure 4-6. BSEC is a good parameter to compare fuel economy of different fuels especially when the densities and energy content of the fuels are different. It can be observed from Figure 4-6 that as the speed increased the BSEC reduced for all the test fuels. DTPO20 had the lowest average energy consumption (21.53 MJ/kWh) followed by Petro-diesel fuel (22.03 MJ/kWh) then DTPO40 (22.11 MJ/kWh) and DTPO 60 (22.09 MJ/kWh). However, based on the average values, these differences were not significant. It was noted that, since fuel is supplied to the engine volumetrically, heating value on volume basis is a good indicator of fuel consumption and economy (Martínez *et al.*, 2013). On volume basis, the heating values of Petro-diesel fuel and DTPO were 38 MJ/L and 39.5 MJ/L respectively which show a small difference. The difference will be lesser for the blends of the two fuels and this explains the minor difference in fuel consumption.
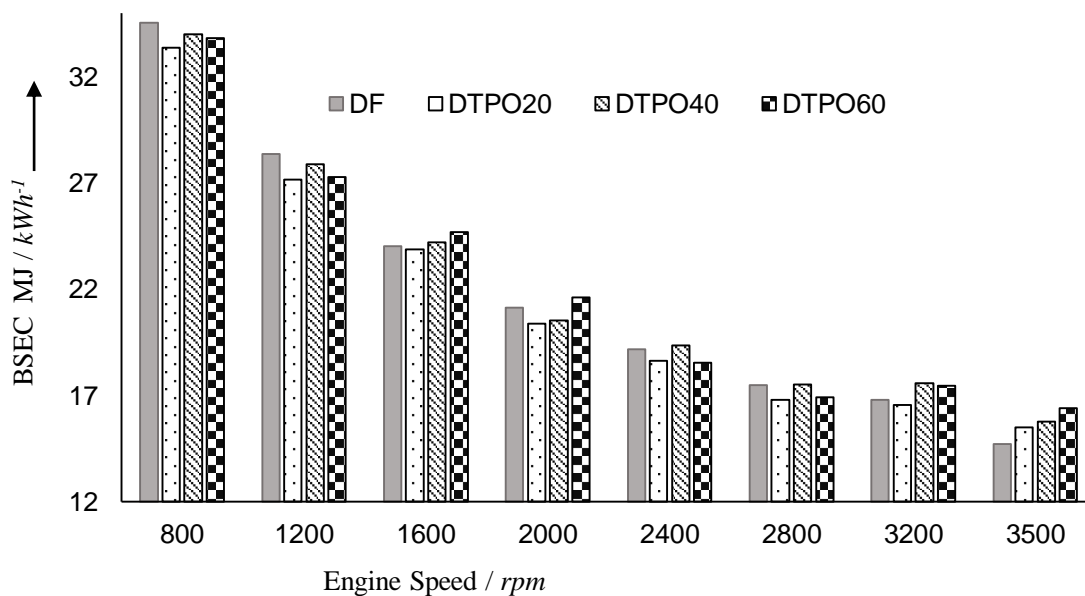


Figure 4-6 Variation of Brake Specific Energy Consumption (BSEC) with engine speed

### 4.2.2 Effects of DTPO/Petro-diesel fuel blends on Exhaust emission

Unburned hydrocarbons (HC) consist of hydrocarbon fuel that is not completely burned (Naima & Liazid, 2013, Pundir, 2007), therefore, it is a result of incomplete combustion. The variation of HC with speed for DTPO/petro-diesel fuel blends is illustrated in Figure 4-7. Petro-diesel fuel had the lowest HC compared to the blends at all the test speeds. At the same time, HC increased with an increase in the concentration of DTPO in the blends. Usually, high density, high viscosity and high aromatic hydrocarbons can lead to incomplete combustion resulting in an increase in unburned hydrocarbons as reported elsewhere (Murugan *et al.*, 2009, Aydın & İlkılıç, 2015). Fuel is supplied to the engine volumetrically, thus, when the density is high, the mass of the fuel being injected into the cylinder increases. Therefore, the high density of DTPO may lead to a rich mixture and, thus, to incomplete combustion. Viscosity is responsible for the quality of spray and mixing of fuel in the combustion chamber. The high viscosity of DTPO could also have led to poor penetration and mixing of fuel into the combustion chamber leading to incomplete combustion. Thus, any factor that can cause incomplete combustion can lead to a rise in the formation of unburned hydrocarbons.
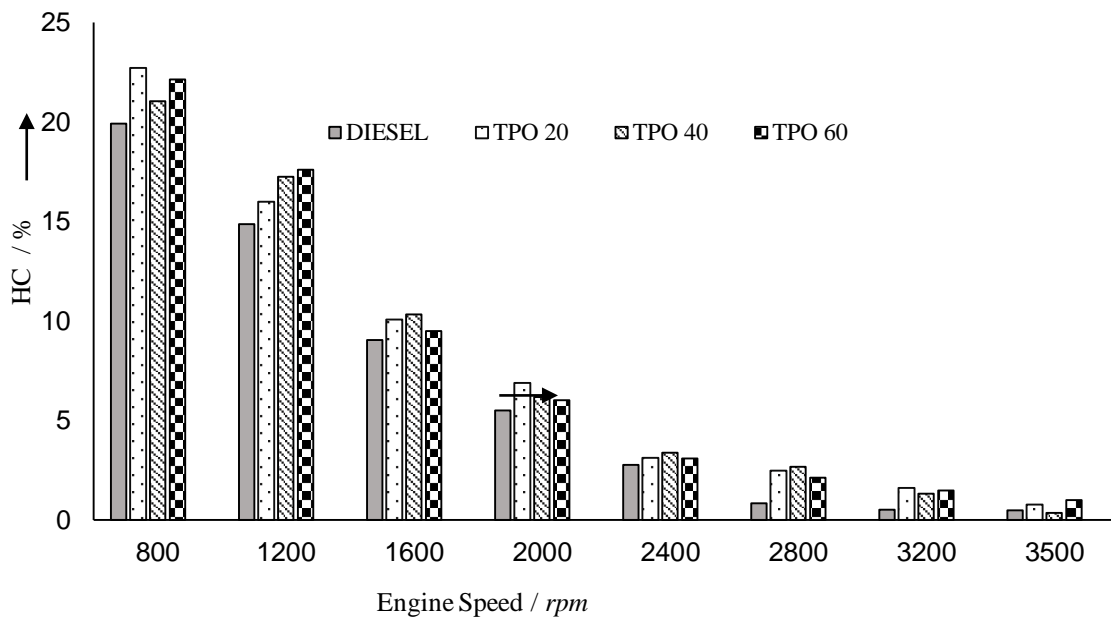
Figure 4-7 Variation of HC with speed

Carbon monoxide (CO) is an odourless and highly toxic gas. It results from insufficient oxygen in the air/fuel mixture during combustion (Pundir, 2007). The effects of Petro-diesel fuel and Petro-diesel fuel/DTPO blends on CO and speed are shown in Figure 4-8. It was observed that the CO increased with the increase in speed. In addition, the average CO emissions for Petro-diesel fuel and DTPO 20 are very comparable, with a difference of 1.3%. DTPO 40 and DTPO 60 were 6.92% and 9.05% higher than the reference petro-diesel fuel. CO emissions depend on air/fuel ratio, a rich mixture increases the formation of CO while in a lean mixture the CO will be oxidised further to $CO_2$. The density of the test fuels increased with increase in DTPO fraction in the blend which could have led to a rich mixture resulting in the incomplete oxidation of CO.
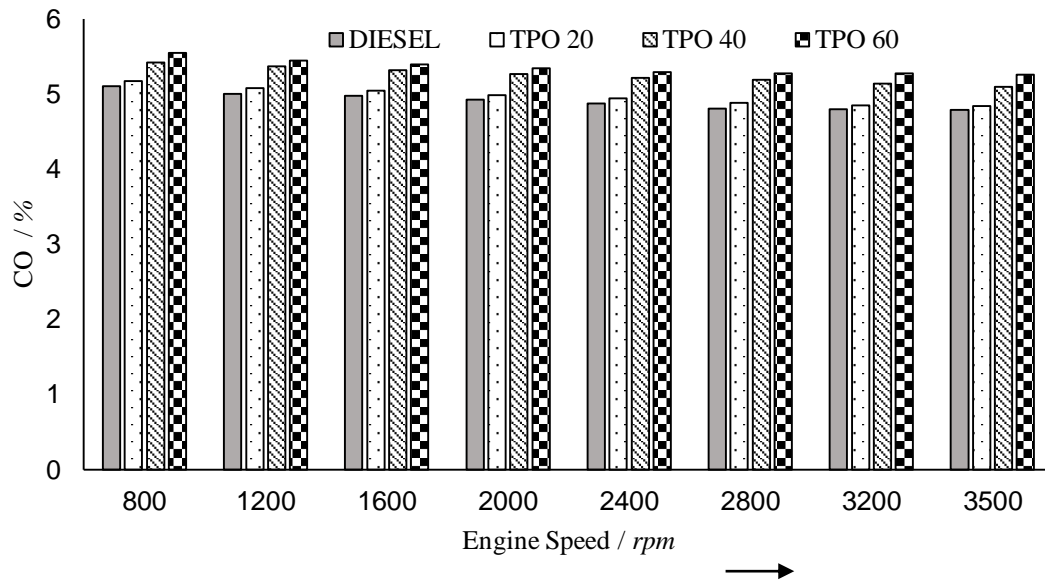
Figure 4-8 Variation of CO with speed

Nitrogen Oxides ($NO_x$) consist mainly of Nitrogen oxide NO and small amounts of Nitrogen dioxide $NO_2$. Variation of $NO_x$ with speed for the test fuels is shown in Figure 4-9. Over the entire speed range, petro-diesel fuel had the highest $NO_x$ emissions. Unlike CO and HC, $NO_x$ is a result of complete combustion (Pundir, 2007). The rate of $NO_x$ formation is highest under conditions of high in-cylinder temperature and oxygen concentration (Pundir, 2007). The amount of $NO_x$ was found to reduce with increase of DTPO content in the oil. This could be attributed to higher rate of heat release for petro-diesel fuel compared to the blends which in turn results in an increase in formation of $NO_x$. This was confirmed in Figure 4-10, as shall be discussed later, where the peak pressure was highest for petro-diesel fuel compared to the blends of DTPO.
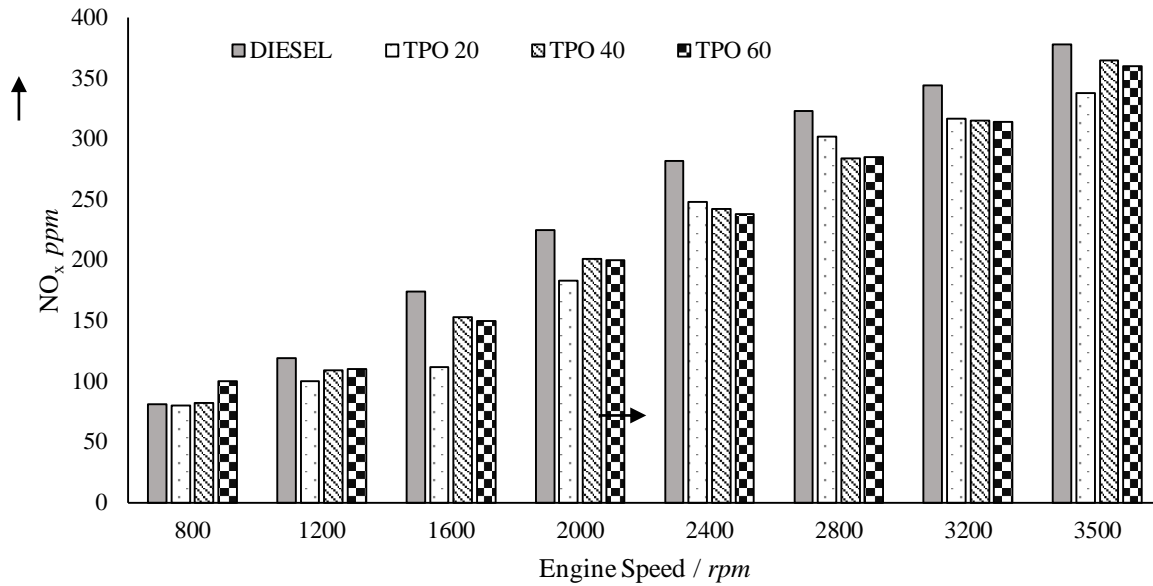
Figure 4-9 Variation of NOx with speed

### 4.2.3 Effects of DTPO/Petro-diesel fuel blends on Combustion characteristics of the diesel engine

The variation of peak pressure with speed is illustrated in Figure 4-10 while the rate of pressure rise with crank angle at an engine speed of 3200 rpm is shown in Figure 4-11. Peak pressure for petro-diesel fuel varied from 77.46 bar at 800 rpm to 47.83 bar at 3200 rpm. Whereas that for DTPO20 varied from 77.96 bar at 800 rpm to 47.06 bar at 3200 rpm. For DTPO 40, the peak pressure varied from 75.01 bar at 800 rpm to 44.22 bar at 3200 rpm. Finally, the Peak pressure for DTPO60 changed from 75.15 bar at 800 rpm to 44.23 bar at 3200 rpm. On average, the pressures were 66.57 bar, 66.01 bar, 65.74 bar and 65.08 bar for Petro-diesel fuel, DTPO20, DTPO40 and DTPO 60 respectively. Though the differences in peak pressure were not significant, they tended to reduce with the concentration of DTPO in the blend.

Pressure rise is determined by the first two stages of combustion. The first stage is the ignition delay, where the fuel injected is broken down to droplets and mix with air, and the next stage is where the fuel prepared during the ignition delay burns leading to a high rise in pressure up

to a maximum point (Benson & Whitehouse, 1983). From Figure 4-10, the peak pressure of petro-diesel fuel was highest compared to those of the other blends. From Figure 4-11, it can be seen that, the combustion of Petro-Diesel took place earlier compared to the blends DTPO20, DTPO40 and DTPO 60 in that order. It can also be noted that the ignition delay of the fuels increased with an increase in concentration of DTPO in the blend as shown in Figure 4-11. Ordinarily, when the ignition delay is longer, there is an increase in the quantity of fuel in the combustion chamber which will have time to mix with air and be more homogeneous. Subsequently when the accumulated fuel ignites, it will burn rapidly leading to a rise in temperature and high peak pressure (Aydın & İlkılıç, 2015, Murugan *et al.*, 2009). However, the test fuels exhibited the opposite behaviour. This observation could be due to the inefficient combustion of DTPO due to the high viscosity and its poor ignition quality. Aromatic content of TPO is normally high and fuels with high aromatic content have poor ignition quality (Aydın & İlkılıç, 2015, Murugan *et al.*, 2009).
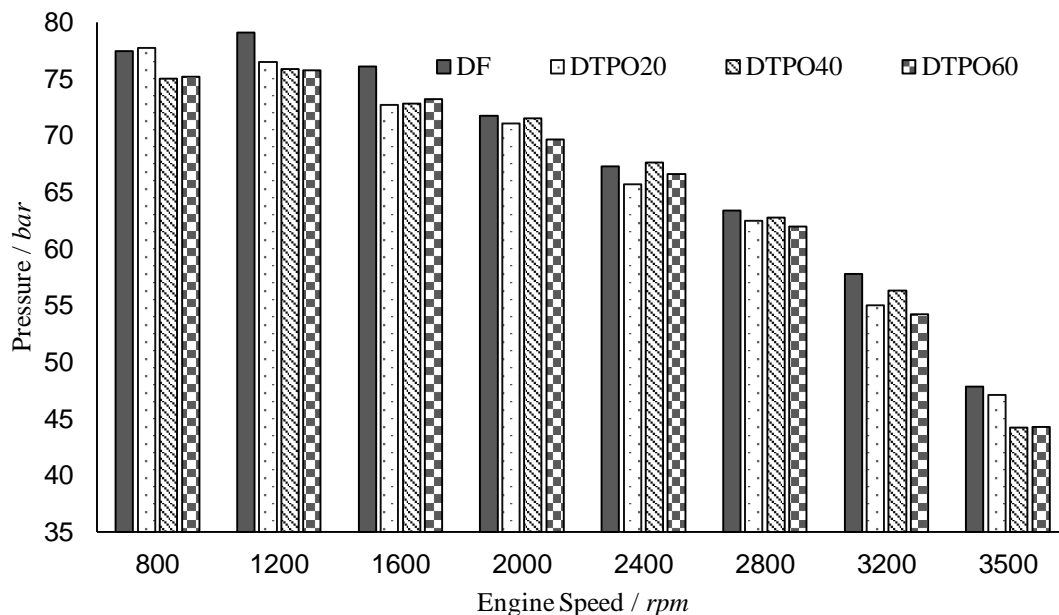


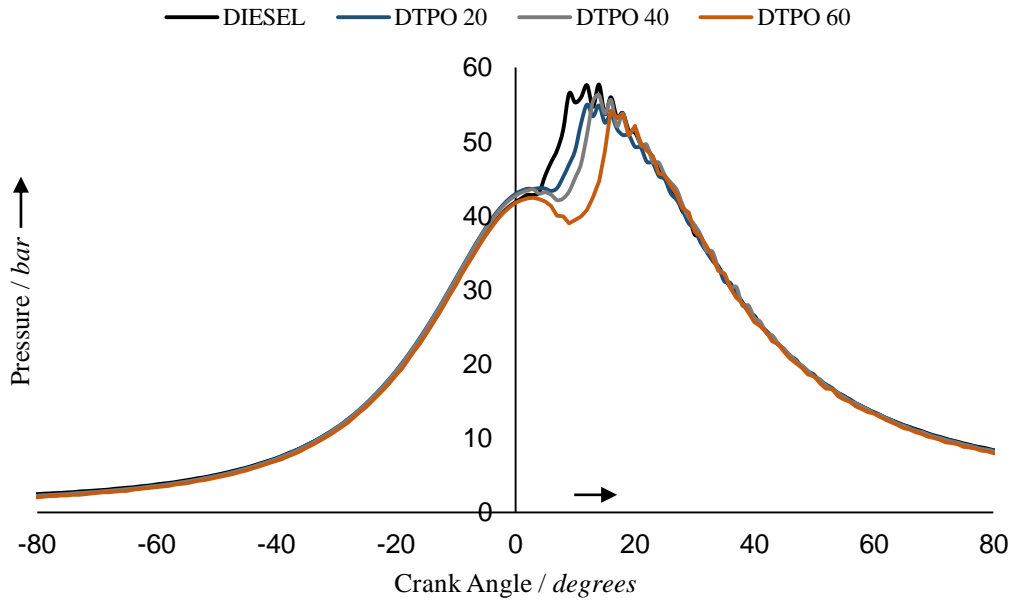Figure 4-10 Variation of peak pressure with engine speed

Figure 4-11 Variation of in cylinder pressure with crank angle at 3200 rpm

## 4.3    Prediction of engine performance using Artificial Neural Network

The ANN model was created with the aim of predicting Power, torque, SFC and peak pressure based on DTPO blend concentration and engine speed. As mentioned previously, the goal was to maximise the correlation coefficient (R). The model had three layers. Input, output and one hidden layer. The logsig was used in the hidden layer while the purelin was used in the output layer. The optimum number of neurons was found to be 10. As seen in Table 4-5, there was no improvement in R when the number of neurons was increased beyond 10. But there was a drop in the R value when the number of neurons was below 10. The Mean Square Error (MSE) was found to be 0.000396 for this network.  So based on this analysis, a network with 10 neurons was selected as the optimum network. The correlation coefficient for the training, validation and testing data sets was found to be 0.99476, 0.99606 and 0.99699. That for the whole network was 0.99519. The high correlation by the ANN model indicates that the model can predict the engine performance adequately.

Table 4-5 Evaluation of network performance

| neurons | train | valid | test | all | MSE |
|---|---|---|---|---|---|
| 8 | 0.98339 | 0.99357 | 0.99276 | 0.98907 | 0.001146 |
| 10 | 0.99476 | 0.99606 | 0.99699 | 0.99519 | 0.000396 |
| 12 | 0.99575 | 0.99187 | 0.99725 | 0.99526 | 0.000768 |
| 14 | 0.9968 | 0.99751 | 0.96511 | 0.99181 | 0.000365 |
| 16 | 0.98491 | 0.994779 | 0.99167 | 0.98746 | 0.000242 |

To analyse the model further, a regression analysis of the predicted Power, torque, SFC and peak pressure, and the measured experimental values were carried out and the results are shown in Figure 4-12 to Figure 4-15. From these figures, it is important to note that the predicted values are very close to experimental values, all with R higher than 0.99. The highest accuracy was noted in prediction of power with an R value of 0.9988, then followed by SFC (0.9852) then peak pressure (0.98).
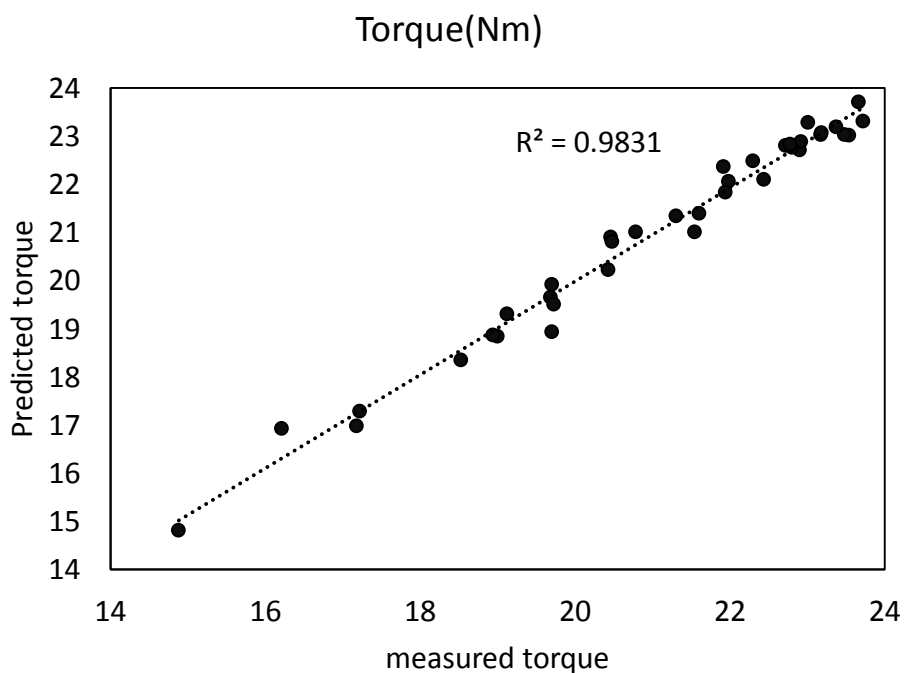


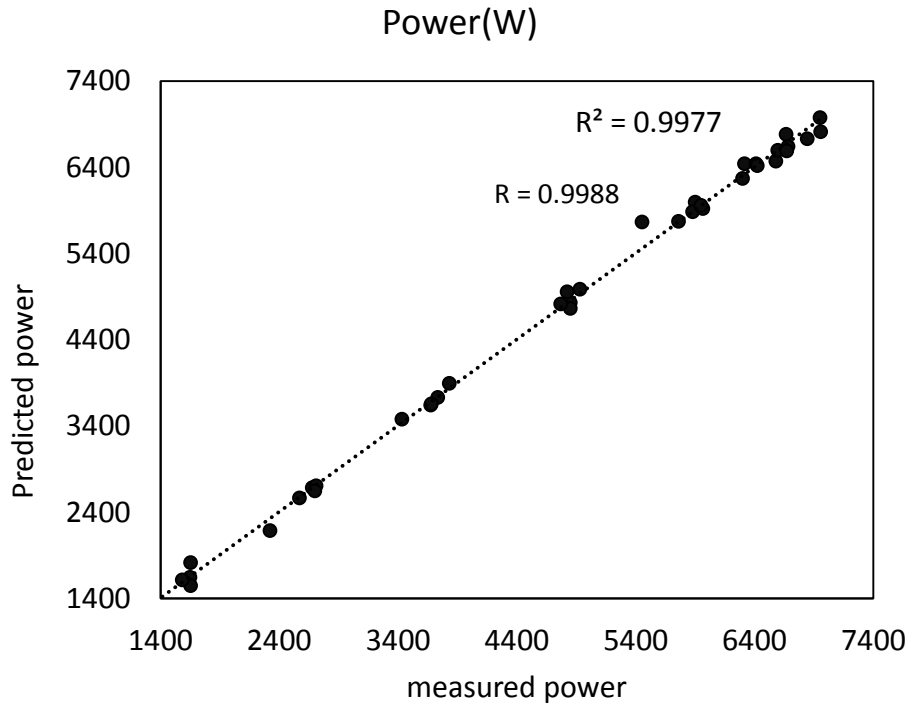Figure 4-12 Predicted and the measured values for engine torque

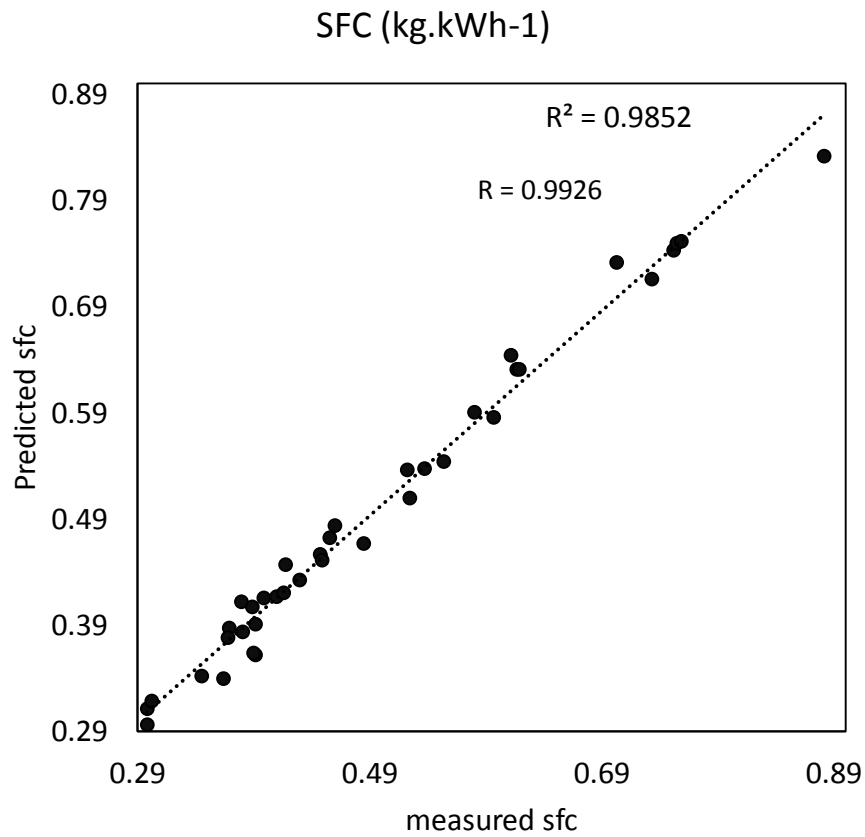Figure 4-13 Predicted and measured values for engine power



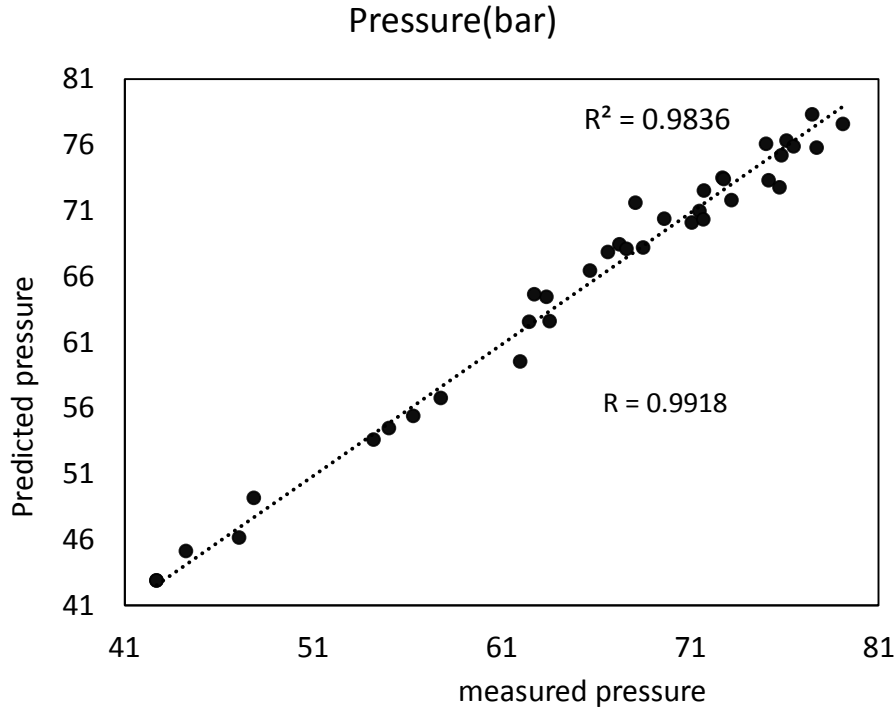Figure 4-14 Predicted vs measured values for SFC

Figure 4-15 Predicted and measured values of peak pressure

Using the weights and biases of the trained ANN model presented on Table 4-6, equations 4-5 to 4-8 for predicting Torque, Power, SFC and Peak pressure were developed. Where $F_r$ and $n_r$ are defined by 4-9 and 4-10 respectively.

$$Torque = -0.62824\, F_1 - 2.27774F_2 - 4.95962F_3 - 3.15835F_4 +$$
$$2.396874F_5 - 0.68893F_6 - 0.66841F_7 + 1.148365F_8 + 0.94004F_9 -$$
$$0.77478\, F_{10} + 3.11982 \qquad\qquad\qquad 4\text{-}5$$

$$Power = -0.39857F_1 - 0.99469F_2 - 1.74611F_3 - 1.15229F_4 + 0.664703F_5 -$$
$$0.17873F_6 - 2.29807F_7 + 0.389097F_8 + 0.29911F_9 - 0.39475F_{10} + 2.459376$$
$$4\text{-}6$$

$$sfc = 0.687379F_1 + 1.158229F_2 + 4.013523F_3 + 2.364102F_4 + 0.544825F_5 +$$
$$0.128098F_6 + 0.39712F_7 + 0.503372F_8 \pm 0.31545F_9 + 0.410813F_{10} - 4.34864$$

$$Pressure = -4.87243F_1 - 6.89962F_2 + 0.40131F_3 + 0.791098F_4 + 2.109962F_5 -$$

$$0.00679F_6 + 0.602341F_7 + 1.305551F_8 + 0.71885F_9 - 0.42125F_{10} + 2.429029$$

*4-8*

$$F_R = \frac{1}{1 - e^{-n_R}}$$   *4-9*

$$n_R = (\%DTPO)W_{1R} + (RPM)W_{2R} + b_R$$   *4-10*

Table 4-6 Weights between input and hidden layer for engine performance network

| R | $W_{1R}$ | $W_{2R}$ | $b_R$ |
|---|---|---|---|
| 1 | -9.76025 | -12.4795 | 14.54184 |
| 2 | 6.648437 | 7.144041 | -9.16342 |
| 3 | 1.979585 | -2.15947 | -2.53553 |
| 4 | -3.49731 | 1.656516 | 2.546858 |
| 5 | 2.986831 | -0.98879 | 2.189052 |
| 6 | 6.245957 | 4.506771 | -0.95217 |
| 7 | 0.01654 | -2.35417 | -0.17246 |
| 8 | -9.31786 | 0.50364 | -5.47606 |
| 9 | -0.14736 | 10.10856 | -8.31487 |
| 10 | -5.19179 | -7.23604 | -10.3794 |

## 4.4   Prediction of engine emissions using Artificial Neural Network

A network with one hidden layer was developed to predict HC, CO and NOx. The optimum

number of neurons in the hidden layer was found to be 10. The correlation coefficient did not

increase beyond 10 neurons. Subsequently, a network with 10 neurons was considered

satisfactory. The proposed ANN model for predicting HC, CO and NOx had correlation

coefficients of 0.99761, 0.991 and 0.99552 for training, test and validation data sets

respectively. The correlation coefficient for the whole network was 0.9975. Additionally, the

MSE was 0.000163, that shows that the network was able to learn the relationship between the input and output parameters reasonably well.

To further evaluate the prediction ability of the ANN, regression curves were plotted for the predicted vs measured HC, CO and NOx values as shown in Figure 4-16 to Figure 4-18. It was found that the $R^2$ values for HC, O and NOx were 0.9961, 0.9921 and 0.997 respectively. Based on the high $R^2$ values it can be concluded that the model was able to generalise between the input parameters of engine speed and DTPO blend concentration and the emissions satisfactorily.
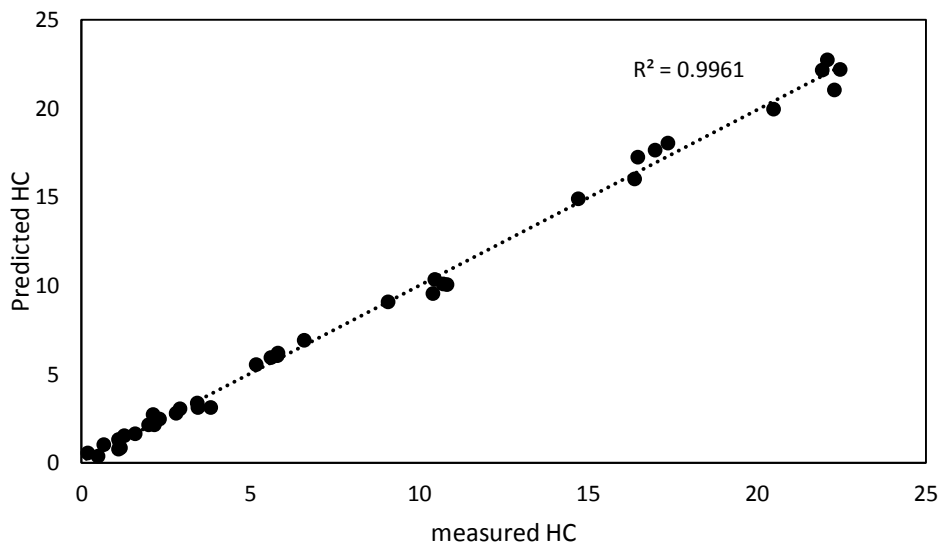


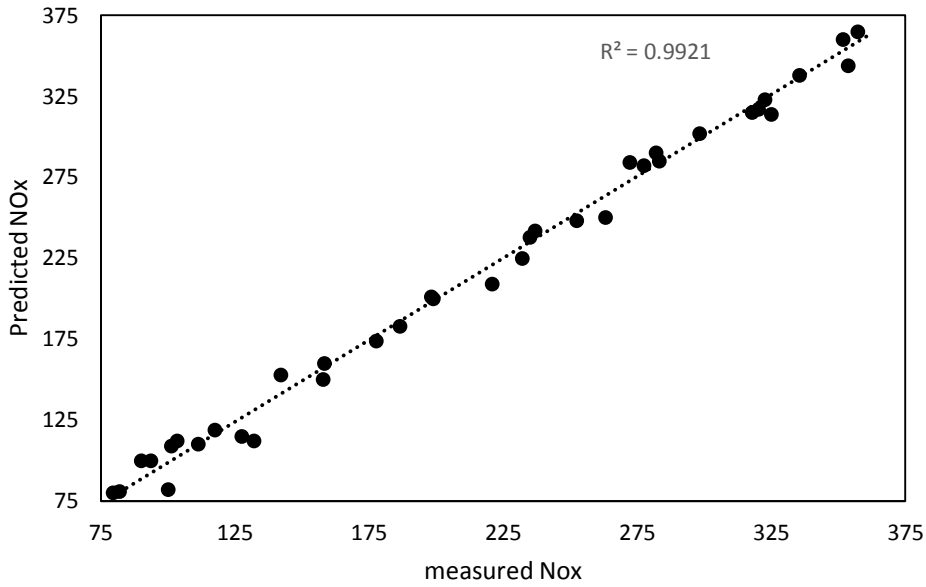Figure 4-16 predicted and measured values for HC

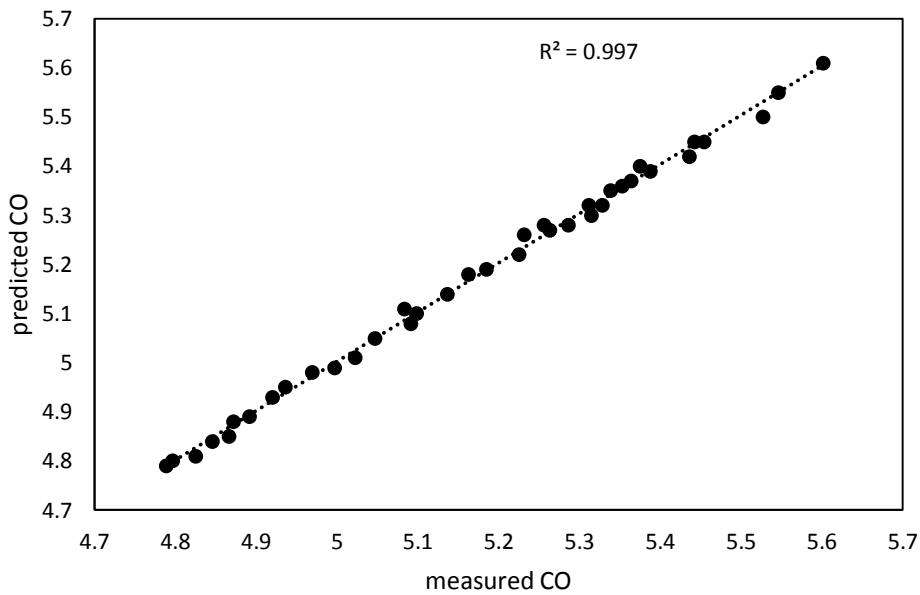Figure 4-17 Predicted and measured values for NOx



Figure 4-18 predicted and measured values for CO

Using the weights and biases of the trained ANN model presented on Table 4-7. Equations 4-11 to 4-13 were developed for predicting HC, CO and NOx respectively. Where $F_R$ and $n_R$ are defined by 4-14 and 4-15 respectively.

Table 4-7 Weights between input and hidden layer for engine performance network

| r | $W_{1r}$ | $W_{2r}$ | $b_r$ |
|---|---|---|---|
| 1 | -1.79787 | 7.87059 | 7.152767 |
| 2 | -7.22874 | 2.27573 | 6.371598 |
| 3 | -6.97209 | -5.94619 | 5.622027 |
| 4 | -8.89691 | -1.8935 | 0.869408 |
| 5 | -4.63349 | -6.23566 | -1.68392 |
| 6 | -0.57759 | 4.088858 | 2.202833 |
| 7 | -3.61501 | 3.704252 | -1.93043 |
| 8 | -9.88563 | 1.215642 | -1.97992 |
| 9 | -4.59867 | -5.96368 | -5.77231 |
| 10 | 9.964487 | -4.79473 | 10.47497 |

$$HC = -0.36519F_1 + 0.065603F_2 + 0.071209F_3 + 0.032547F_4 + 0.154972F_5$$
$$- 1.48203F_6 - 0.23816F_7 + 0.112772F_8 + 0.058713F_9 + 0.165329F_{10}$$
$$+ 0.754924$$

4-11

$$NOx = -0.34459F_1 + 0.237247F_2 - 0.55315F_3 + 0.059885F_4 - 0.44424F_5 + 0.698149F_6$$
$$+ 0.751985F_7 - 0.11371F_8 - 0.03451F_9 - 0.30068F_{10} + 0180492$$

4-12

$$NOx = -0.26591F_1 - 0.23792F_2 + 0.091302F_3 - 0.1377F_4 + 0.126094F_5 -$$
$$0.15905F_6 - 0.26941F_7 - 0.71392F_8 - 0.02062F_9 + 0.190374F_{10} + 0.68119$$

*4-13*

$$F_r = \frac{1}{1 - e^{-n_r}}$$ 

*4-14*

$$n_r = (\%DTPO)W_{1r} + (RPM)W_{2r} + b_r$$

*4-15*

# 5 GENERAL CONCLUSIONS

This study was carried out to evaluate the technical feasibility of using the fraction of tyre pyrolysis oil that has the same typical distillation range as diesel fuel. Basic properties of the fuel were determined and the performance, emission and combustion characteristics of the fuel and its blends with petro-diesel fuel were experimentally evaluated. An ANN model was developed to predict engine performance and emissions based on fuel blends. From the findings of this work, the following conclusions are made:

- The viscosity, density, copper strip corrosion of DTPO were found to be within the acceptable limits set by SANS-342, while the sulphur content and flash point were out of these limits.

- The viscosity and density of DTPO and its blends with petro-diesel fuel at various temperatures between 20 °C – 100 °C can be estimated using the equations developed with an acceptable level of accuracy.

- Distilling TPO had an effect on most of the properties. For instance the viscosity of DTPO was lower than that of TPO and closer to that of petro-diesel fuel. The energy content of DTPO on volume basis was higher compared to petro-diesel fuel and TPO. There was a 22% reduction in sulphur content after distilling TPO. The flash point of DTPO was higher than that of TPO. The only property that was not affected was the density.

- The engine was able to run without any operational problems with blends of up to 60% DTPO. When the blend concentration was increased to 80%, the engine operation became unstable.

- There was no significant difference in BSEC for the test fuels. The lowest BSEC was obtained for DTPO20. There was no significant difference in power and torque up to a

speed of 2800 rpm. Beyond this speed, the power reduced with increase in DTPO in the blend. Therefore, the performance of the engine was slightly lower when the DTPO was increased.

- HC and CO increased with the concentration of DTPO in the test fuels, while $NO_x$ reduced with DTPO concentration. These observations were attributed to Petro-diesel fuel having better combustion characteristics due to its lower viscosity, density and better ignition quality.

- Petro-diesel fuel's peak pressure was high compared to those of the blends. It was also found that the ignition delay of the blends of DTPO was longer than that of petro-diesel fuel due to the aromatic nature of TPO which in turn reduced its ignition quality.

- Engine performance and emissions can be predicted reasonably well using the ANN models that were developed. There was a strong correlation between ANN predicted values and experimental values. The ANN successfully predicted four engine performance outputs and three exhaust emission parameters. Therefore, the developed model can be used to predict engine performance and emission of a diesel engine running on various blends of DTPO and petro-diesel fuel at different engine speeds.

## 6 LIMITATIONS

The ANN model developed and validated in this work is limited to predicting engine performance when running on DF/DTPO blends with upto 60% DTPO concentration. Therefore it may not be suitable for extrapolation beyond this limits. The model can only be used for prediction for the specific or similar engine used in this work and not any other type of engine and within the speed of 3500 rpm.

# 7   RECOMMENDATIONS FOR FURTHER STUDIES

Research is a continuous process and with each step, new areas to explore normally come up. There are, therefore, areas that have been identified for further research concerning the use of TPO in diesel engines as highlighted below.

- The sulphur content in this study was found to be high, therefore, different methods of sulphur reduction should be explored to reduce the sulphur content to acceptable limits. As Sulphur is also associated with lubricity of the oil, the effect of Sulphur reduction on lubricity should also be studied.

- One of the main concerns when using alternative fuels in diesel engines is the long term effects on wear and durability of the engine. Therefore, it is recommended that a study on wear and durability of using TPO on diesel engines be studied.

- A model was developed to predict engine performance and emissions based on artificial neural network. It is recommended to use single zone, zero-dimensional and multi-dimensional models to gain a proper insight into the combustion process of the diesel engine running on tyre pyrolysis oil.

# 8 REFERENCES

Alcala, A. & Bridgwater, A. 2013, "Upgrading fast pyrolysis liquids: blends of biodiesel and pyrolysis oil", *Fuel,* vol. 109, pp. 417-426.

Anne & Russ, E. 2006, *The Composition of a Tyre: Typical Components*, The Waste & Resources Action Programme, Banbury Oxford UK.

Aydın, H. & İlkılıç, C. 2015, "Analysis of combustion, performance and emission characteristics of a diesel engine using low sulfur tire fuel", *Fuel,* vol. 143, pp. 373-382.

Aydın, H. & İlkılıç, C. 2012, "Optimization of fuel production from waste vehicle tires by pyrolysis and resembling to diesel fuel by various desulfurization methods", *Fuel,* vol. 102, no. 0, pp. 605-612.

Banar, M., Akyıldız, V., Özkan, A., Çokaygil, Z. & Onay, Ö 2012, "Characterization of pyrolytic oil obtained from pyrolysis of TDF (Tire Derived Fuel)", *Energy Conversion and Management,* vol. 62, pp. 22-30.

Belagur, V.K. & Wadawadagi, S.B. 2009, "Effect of Injection Pressure on Performance, Emission and Combustion Characteristics of Direct Injection Diesel Engine Running on Blends of Pongamia Pinnata Linn (Honge oil) Oil and Diesel Fuel", *Agricultural Engineering International: CIGR Journal, Vol.6, pp. 1-17.*

Benallal, B., Roy, C., Pakdel, H., Chabot, S. & Poirier, M. 1995, "Characterization of pyrolytic light naphtha from vacuum pyrolysis of used tyres comparison with petroleum naphtha", *Fuel,* vol. 74, no. 11, pp. 1589-1594.

Benson, R. & Whitehouse, N.D. 1983, *Internal combustion engines:a detailed introduction to the thermodynamics of spark and compression ignition engines, their design and development,* Pergamon Press, Oxford.

Bhatt, P. & Patel, P. 2012, "Suitability of Tyre Pyrolysis Oil (TPO) as an Alternative Fuel for Internal Combustion Engine", *International Journal of Advanced Engineering Research Studies,* , pp. 61-65.

Bietresato, M., Calcante, A. & Mazzetto, F. 2015, "A neural network approach for indirectly estimating farm tractors engine performances", *Fuel,* vol. 143, pp. 144-154.

Canakci, M., Ozsezen, A.N., Arcaklioglu, E. & Erdil, A. 2009, "Prediction of performance and exhaust emissions of a diesel engine fueled with biodiesel produced from waste frying palm oil", *Expert Systems with Applications,* vol. 36, no. 5, pp. 9268-9280.

Celik, V. & Arcaklioğlu, E. 2005, "Performance maps of a diesel engine", *Applied Energy,* vol. 81, no. 3, pp. 247-259.

Centeno, G., Sánchez-Reyna, G., Ancheyta, J., Muñoz, J.A. & Cardona, N. 2011, "Testing various mixing rules for calculation of viscosity of petroleum blends", *Fuel,* vol. 90, no. 12, pp. 3561-3570.

Chaala, A. & Roy, C. 1996, "Production of coke from scrap tire vacuum pyrolysis oil", *Fuel Processing Technology,* vol. 46, no. 3, pp. 227-239.

de Marco Rodriguez, I., Laresgoiti, M.F., Cabrero, M.A., Torres, A., Chomón, M.J. & Caballero, B. 2001, "Pyrolysis of scrap tyres", *Fuel Processing Technology,* vol. 72, no. 1, pp. 9-22.

Demirbas, A. 2008, "Distillation properties of various diesel oils", *Energy Sources, Part A,* vol. 30, no. 16, pp. 1484-1490.

Demuth, H. & Beale, M. 2001, "Neural network toolbox for use with MATLAB", The MathWorks, Inc.

Dhole, A., Yarasu, R., Lata, D. & Baraskar, S. 2014, "Mathematical modeling for the performance and emission parameters of dual fuel diesel engine using hydrogen as secondary fuel", *International Journal of Hydrogen Energy,* vol. 39, no. 24, pp. 12991-13001.

Doğan, O., Çelik, M.B. & Özdalyan, B. 2012, "The effect of tire derived fuel/diesel fuel blends utilization on diesel engine performance and emissions", *Fuel,* vol. 95, pp. 340-346.

Eastop, T. & McConkey, A. 5$^{th}$ Edition, 1993, "Applied thermodynamics for engineering technologists" Pearson Education Limited. London.

Edwin Raj, R., Robert Kennedy, Z. & Pillai, B. 2013, "Optimization of process parameters in flash pyrolysis of waste tyres to liquid and gaseous fuel in a fluidized bed reactor", *Energy Conversion and Management,* vol. 67, pp. 145-151.

Encyclopaedia Britannica. Volume 16. 15$^{th}$ edition. Helen Hemingway Benton publisher. 1974.

Enweremadu, C. & Rutto, H. 2010, "Combustion, emission and engine performance characteristics of used cooking oil biodiesel—A review", *Renewable and Sustainable Energy Reviews,* vol. 14, no. 9, pp. 2863-2873.

Frigo, S., Seggiani, M., Puccini, M. & Vitolo, S. 2014, "Liquid fuel production from waste tyre pyrolysis and its utilisation in a Diesel engine", *Fuel,* vol. 116, pp. 399-408.

Ghobadian, B., Rahimi, H., Nikbakht, A., Najafi, G. & Yusaf, T. 2009, "Diesel engine performance and exhaust emission analysis using waste cooking biodiesel fuel with an artificial neural network", *Renewable Energy,* vol. 34, no. 4, pp. 976-982.

Hansdah, D., Murugan, S. & Das, L. 2013, "Experimental studies on a DI diesel engine fueled with bioethanol-diesel emulsions", *Alexandria Engineering Journal,* vol. 52, no. 3, pp. 267-276.

Hansen, A.C., Zhang, Q. & Lyne, P.W. 2005, "Ethanol–diesel fuel blends—a review", *Bioresource technology,* vol. 96, no. 3, pp. 277-285.

Hariharan, S., Murugan, S. & Nagarajan, G. 2013, "Effect of diethyl ether on Tyre pyrolysis oil fueled diesel engine", *Fuel,* vol. 104, pp. 109-115.

Hossain, A. & Davies, P. 2013, "Pyrolysis liquids and gases as alternative fuels in internal combustion engines–A review", *Renewable and sustainable energy reviews,* vol. 21, pp. 165-189.

Ilangkumaran, M., Sakthivel, G. & Nagarajan, G. 2016, "Artificial neural network approach to predict the engine performance of fish oil biodiesel with diethyl ether using back propagation algorithm", *International Journal of Ambient Energy,* vol. 37, no. 5, pp. 446-455.

İlkılıç, C. & Aydın, H. 2011, "Fuel production from waste vehicle tires by catalytic pyrolysis and its application in a diesel engine", *Fuel Processing Technology,* vol. 92, no. 5, pp. 1129-1135.

Islam, M., Khan, M. & Alam, M. 2003, "Production and characterization of scrap tyre pyrolysis oil and its blend", *Proceedings of the International Conference on Mechanical Engineering*, *26-28 December, Dhoka Bangladesh.*

Ismail, H.M., Ng, H.K., Queck, C.W. & Gan, S. 2012, "Artificial neural networks modelling of engine-out responses for a light-duty diesel engine fuelled with biodiesel blends", *Applied Energy,* vol. 92, pp. 769-777.

Jaichandar, S. & Annamalai, K. 2013, "The status of biodiesel as an alternative fuel for diesel engine–an overview", *Journal of Sustainable Energy & Environment,* vol. 2, no. 2, pp. 71-75.

Jianmin, L., Xiaolei, L., Xiaoming, Z., Shiyong, X. & Lijun, D. 2011, "Misfire diagnosis of diesel engine based on rough set and neural network", *Procedia Engineering,* vol. 16, pp. 224-229.

Kar, Y. 2011, "Catalytic pyrolysis of car tire waste using expanded perlite", *Waste Management,* vol. 31, no. 8, pp. 1772-1782.

Khan, Z. & Ali, S. 2013, "Oxidative desulphurization followed by catalytic adsorption method", *South African Journal of Chemical Engineering,* vol. 18, no. 2, pp. 14-28.

Koc, A.B. & Abdullah, M. 2014, "Performance of a 4-cylinder diesel engine running on tire oil–biodiesel–diesel blend", *Fuel Processing Technology,* vol. 118, pp. 264-269.

Kumar, G., Srinivas, G. & Ch, A.K. 2012, "Experimental Investigations on Diesel Engine Fueled with Tyre Pyrolysis Oil and Diesel Blends", *International Journal of Emerging Trends in Engineering and Developement,* vol. 7, no. 2, pp. 98-105.

Laresgoiti, M., Caballero, B., de Marco, I., Torres, A., Cabrero, M. & Chomón, M. 2004, "Characterization of the liquid products obtained in tyre pyrolysis", *Journal of Analytical and Applied Pyrolysis,* vol. 71, no. 2, pp. 917-934.

Martínez, J.D., Lapuerta, M., García-Contreras, R., Murillo, R. & García, T. 2013, "Fuel properties of tire pyrolysis liquid and its blends with diesel fuel", *Energy & Fuels,* vol. 27, no. 6, pp. 3296-3305.

Martínez, J.D., Puy, N., Murillo, R., García, T., Navarro, M.V. & Mastral, A.M. 2013, "Waste tyre pyrolysis–A review", *Renewable and Sustainable Energy Reviews,* vol. 23, pp. 179-213.

Martínez, J.D., Rodríguez-Fernández, J., Sánchez-Valdepeñas, J., Murillo, R. & García, T. 2014, "Performance and emissions of an automotive diesel engine using a tire pyrolysis liquid blend", *Fuel,* vol. 115, pp. 490-499.

Mohammadhassani, J., Dadvand, A., Khalilarya, S. & Solimanpur, M. 2015, "Prediction and reduction of diesel engine emissions using a combined ANN-ACO method", *Applied Soft Computing, Vol 34. pp 139-150* .

Murillo, R., Aranda, A., Aylón, E., Callén, M.S. & Mastral, A.M. 2006, "Process for the separation of gas products from waste tire pyrolysis", *Industrial & Engineering Chemistry Research,* vol. 45, no. 5, pp. 1734-1738.

Murugan, S., Ramaswamy, M. & Nagarajan, G. 2008a, "A comparative study on the performance, emission and combustion studies of a DI diesel engine using distilled tyre pyrolysis oil–diesel blends", *Fuel,* vol. 87, no. 10, pp. 2111-2121.

Murugan, S., Ramaswamy, M. & Nagarajan, G. 2008b, "The use of tyre pyrolysis oil in diesel engines", *Waste Management,* vol. 28, no. 12, pp. 2743-2749.

Murugan, S., Ramaswamy, M.C. & Nagarajan, G. 2009, "Assessment of pyrolysis oil as an energy source for diesel engines", *Fuel Processing Technology,* vol. 90, no. 1, pp. 67-74.

Mwasiagi, J.I., Huang, X. & Wang, X. 2008, "Performance of neural network algorithms during the prediction of yarn breaking elongation", *Fibers and Polymers,* vol. 9, no. 1, pp. 80-86.

Naima, K. & Liazid, A. 2013, "Waste oils as alternative fuel for diesel engine: A review", *Journal of Petroleum Technology and Alternatives Fuels,* vol. 4, pp. 30-43.

Neumann, H., Paczynska-Lahme, B. & Severin, D. 1981, "Composition and properties of petroleum", Halsted Press, New York. NY.

Nikzadfar, K. & Shamekhi, A.H. 2014, "Investigating the relative contribution of operational parameters on performance and emissions of a common-rail diesel engine using neural network", *Fuel,* vol. 125, pp. 116-128.

Nkosi, N., Muzenda, E., Zvimba, J. & Pilusa, J. 2013, "The current waste generation and management trends in South Africa: A Review", *International Conference on Integrated Waste Management and Green Energy Engineering* Planetary Scientific Research Center, Johannesburg (South Africa), April 15-16, pp. 303.

Oğuz, H., Sarıtas, I. & Baydan, H.E. 2010, "Prediction of diesel engine performance using biofuels with artificial neural network", *Expert Systems with Applications,* vol. 37, no. 9, pp. 6579-6586.

Omidvarborna, H., Kumar, A. & Kim, D. 2016, "Artificial neural network prediction of NOx emissions from EGR and non- EGR engines running on soybean biodiesel fuel (B5) during cold idle mode", *Environmental Progress & Sustainable Energy,* vol. 35, no. 5, pp. 1537-1544.

Öztop, H., Varol, Y., Altun, Ş & Firat, M. 2014, "Using Gasoline-like Fuel Obtained from Waste Automobile Tires in a Spark-ignited Engine", *Energy Sources, Part A: Recovery, Utilization, and Environmental Effects,* vol. 36, no. 13, pp. 1468-1475.

Pilusa, J. & Muzenda, E. 2013, "Qualitative analysis of waste rubber-derived oil as an alternative diesel additive", *International Conference on Chemical and Environmental Engineering* International Conference on Chemical and Environmental Engineering (ICCEE'2013), Johannesburg (South Africa), April 15-16, pp. 13.

Pilusa, J., Shukla, M. & Muzenda, E. 2014, "Economic assessment of waste tyres pyrolysis technology: a case study for Gauteng Province, South Africa", International Journal of Research in Chemical, Metallurgy and Civil Engg (IJREMCE) Vol I, pp 41-49.

Pundir, B. 2007, *Engine emissions: pollutant formation and advances in control technology,* Alpha Science International, Limited. Pennsylvania.

Ramos, J.I. 1989, *Internal combustion engine modeling,* Hemisphere publishing corporation.

Rao, K.P., Babu, T.V., Anuradha, G. & Rao, B.A. 2016, "IDI diesel engine performance and exhaust emission analysis using biodiesel with an artificial neural network (ANN)", *Egyptian Journal of Petroleum,* Article in Press. Available: http://dx.doi.org/10.1016/j.ejpe.2016.08.006

Rawlins, M.S. 2005, *Diesel engine performance modelling using neural networks,* Doctoral Dissertation in Mechanical Engineering, Durban University of Technology, Durban,South Africa.

Recycling and Economic Development Initiative of South Africa (REDISA) *, The Waste Tyre Problem.* Available: http://www.redisa.org.za/ [2014, June/08].

Richard, S. 1992, *Introduction to Internal Combustion engines,* second edn, Macmillan Press LTD.

Rotich, N. 2014, "Forecasting of wind speeds and directions with artificial neural networks", Master's Thesis, faculty of Environmental Energy technology, Lappeenranta University of Technology, Finland.

Roy, C., Chaala, A. & Darmstadt, H. 1999, "The vacuum pyrolysis of used tires: End-uses for oil and carbon black products", *Journal of Analytical and Applied Pyrolysis,* vol. 51, no. 1, pp. 201-221.

Roy, C., Darmstadt, H., Benallal, B., Chaala, A. & Schwerdtfeger, A. 1995, "Vacuum pyrolysis of used tires", *Proceedings of the International Conference on Composite Materials and Energy*, pp. 441.

Roy, S., Banerjee, R. & Bose, P.K. 2014, "Performance and exhaust emissions prediction of a CRDI assisted single cylinder diesel engine coupled with EGR using artificial neural network", *Applied Energy,* vol. 119, pp. 330-340.

Selim, M., Ghannam, M., Aldajah, S. & Saleh, H. 2015, "The Effect of Temperature and Mixing on the Density and Viscosity of Jojoba-diesel Fuels", *Energy Sources, Part A: Recovery, Utilization, and Environmental Effects,* vol. 37, no. 16, pp. 1774-1781.

Sharma, A. & Murugan, S. 2013, "Investigation on the behaviour of a DI diesel engine fueled with Jatropha Methyl Ester (JME) and Tyre Pyrolysis Oil (TPO) blends", *Fuel,* vol. 108, pp. 699-708.

Sharma, A., Sahoo, P.K., Tripathi, R. & Meher, L.C. 2016, "Artificial neural network-based prediction of performance and emission characteristics of CI engine using polanga as a biodiesel", *International Journal of Ambient Energy,* vol. 37, no. 6, pp. 559-570.

Silitonga, A., Masjuki, H., Ong, H.C., How, H., Kusumo, F., Teoh, Y. & Mahlia, T. 2015, "Engine Performance, Emission and Combustion in Common Rail Turbocharged Diesel Engine from Jatropha Curcas Using Artificial Neural Network", *Technical Paper,* , pp. 32-0710.

Siwale, L., Kristóf, L., Adam, T., Bereczky, A., Mbarawa, M., Penninger, A. & Kolesnikov, A. 2013, "Combustion and emission characteristics of n-butanol/diesel fuel blend in a turbo-charged compression ignition engine", *Fuel,* vol. 107, pp. 409-418.

Taghavifar, H., Khalilarya, S. & Jafarmadar, S. 2014, "Diesel engine spray characteristics prediction with hybridized artificial neural network optimized by genetic algorithm", *Energy,* vol. 71, pp. 656-664.

Taghavifar, H., Taghavifar, H., Mardani, A., Mohebbi, A., Khalilarya, S. & Jafarmadar, S. 2015, "On the modeling of convective heat transfer coefficient of hydrogen fueled diesel engine as affected by combustion parameters using a coupled numerical-artificial neural network approach", *International Journal of Hydrogen Energy,* vol. 40, no. 12, pp. 4370-4381.

Tan, P., Zhao, J., HU, Z., LOU, D., Du, A. & Du, D. 2013, "Effects of fuel properties on exhaust emissions from diesel engines", *Journal of Fuel Chemistry and Technology,* vol. 41, no. 3, pp. 347-355.

Tosun, E., Aydin, K. & Bilgili, M. 2016, "Comparison of linear regression and artificial neural network model of a diesel engine fueled with biodiesel-alcohol mixtures", *Alexandria Engineering Journal,* vol. 55, no. 4, pp. 3081-3089.

Uzun, A. 2012, "A parametric study for specific fuel consumption of an intercooled diesel engine using a neural network", *Fuel,* vol. 93, pp. 189-199.

Williams, P.T. 2013, "Pyrolysis of waste tyres: A review", *Waste Management,* vol. 33, no. 8, pp. 1714-1728.

Wong, K.I., Wong, P.K., Cheung, C.S. & Vong, C.M. 2013, "Modelling of diesel engine performance using advanced machine learning methods under scarce and exponential data set", *Applied Soft Computing,* vol. 13, no. 11, pp. 4428-4441.

Yasin, M.M., Yusaf, T., Mamat, R. & Yusop, A.F. 2014, "Characterization of a diesel engine operating with a small proportion of methanol as a fuel additive in biodiesel blend", *Applied Energy,* vol. 114, pp. 865-873.

Younus, S.M., Kumar, V.R. & Rao, D.Y.H. 2013, "Performance and Emissions Characterstics of Diesel Engine Fueled With Tyre Pyrolysis Oil&Diesel Blends with Additives", vol. 2, no. 5, pp. 32-37.

Yusaf, T.F., Buttsworth, D., Saleh, K.H. & Yousif, B. 2010, "CNG-diesel engine performance and exhaust emission analysis with the aid of artificial neural network", *Applied Energy,* vol. 87, no. 5, pp. 1661-1669.

Yusaf, T., Yousif, B. & Elawad, M. 2011, "Crude palm oil fuel for diesel-engines: experimental and ANN simulation approaches", *Energy,* vol. 36, no. 8, pp. 4871-4878.